iScience

CellPress

Article

Sox2 Acts in Thalamic Neurons to Control the Development of Retina-Thalamus-Cortex Connectivity

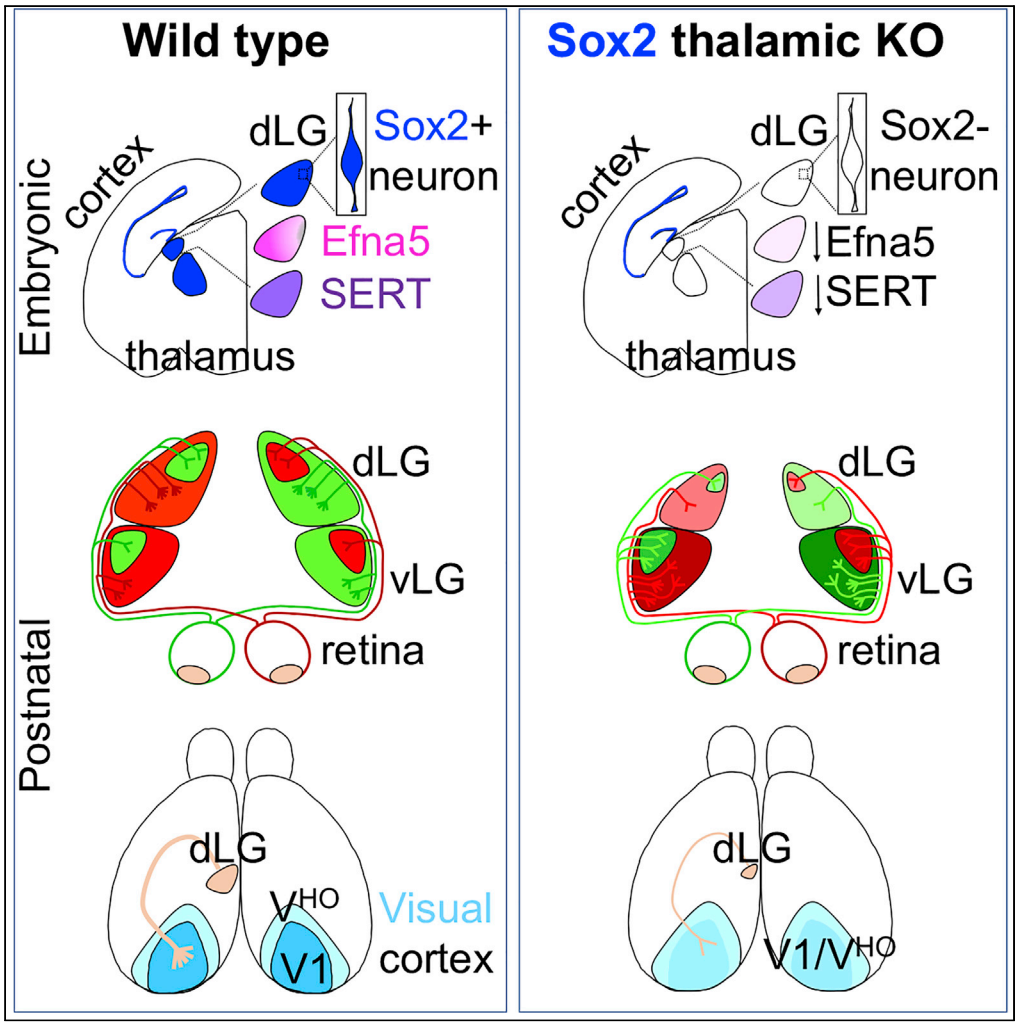

Sara Mercurio, Linda Serra, Alessia Motta, ..., Carolina Frassoni, Paola Bovolenta, Silvia K. Nicolis

silvia.nicolis@unimib.it

HIGHLIGHTS

Sox2 is expressed in postmitotic neurons of the visual thalamic nucleus (dLGN)

Sox2 ablation in the dLGN perturbs retino-thalamic and thalamo-cortical projections

The visual cortex is not correctly patterned in Sox2 thalamic mutants

Downregulation of EphrinA5 and SERT expression may mediate these defects

Mercurio et al., iScience *15*, 257–273
May 31, 2019
https://doi.org/10.1016/j.isci.2019.04.030

iScience

CellPress

Article

Sox2 Acts in Thalamic Neurons to Control the Development of Retina-Thalamus-Cortex Connectivity

Sara Mercurio,[1] Linda Serra,[1,5] Alessia Motta,[1] Lorenzo Gesuita,[1] Luisa Sanchez-Arrones,[3] Francesca Inverardi,[2] Benedetta Foglio,[2] Cristiana Barone,[1] Polynikis Kaimakis,[3] Ben Martynoga,[4] Sergio Ottolenghi,[1] Michèle Studer,[5] Francois Guillemot,[4] Carolina Frassoni,[2] Paola Bovolenta,[3] and Silvia K. Nicolis[1,6,*]

SUMMARY

Visual system development involves the formation of neuronal projections connecting the retina to the thalamic dorso-lateral geniculate nucleus (dLGN) and the thalamus to the visual cerebral cortex. Patients carrying mutations in the *SOX2* transcription factor gene present severe visual defects, thought to be linked to SOX2 functions in the retina. We show that Sox2 is strongly expressed in mouse postmitotic thalamic projection neurons. Cre-mediated deletion of Sox2 in these neurons causes reduction of the dLGN, abnormal distribution of retino-thalamic and thalamo-cortical projections, and secondary defects in cortical patterning. Reduced expression, in mutants, of Sox2 target genes encoding ephrin-A5 and the serotonin transport molecules SERT and vMAT2 (important for establishment of thalamic connectivity) likely provides a molecular contribution to these defects. These findings unveil thalamic SOX2 function as a novel regulator of visual system development and a plausible additional cause of brain-linked genetic blindness in humans.

INTRODUCTION

The development of specific neuron-to-neuron connections is central to the formation and function of the nervous system. In the mammalian visual system, the retina sends visual information to the thalamic dorso-lateral geniculate nucleus (dLGN); the dLGN neurons in turn connect to the visual cerebral cortex, which elaborates visual information. In development, retinal axons, forming the optic nerve, outgrow toward the dLGN, and then generate connections with a precise spatial distribution, linking retinal projections from each specific eye to specific dLGN subregions, in response to region-specific signals produced by the dLGN. In turn, dLGN neurons develop precise connections to the visual cerebral cortex (Garel and Lopez-Bendito, 2014; Gezelius and Lopez-Bendito, 2017). The gene regulatory networks active in dLGN neurons, specifying their connectivity programs, are still poorly understood, and are being investigated (Gezelius and Lopez-Bendito, 2017; Horng et al., 2009).

In humans, mutations in the gene encoding the Sox2 transcription factor cause severe visual disease (Fantes et al., 2003; Williamson and FitzPatrick, 2014). Conditional eye-specific knockout (KO) in mouse showed that, in the visual system, Sox2 plays important functions in retinal and lens progenitor cells' development (Pevny and Nicolis, 2010; Taranova et al., 2006; Smith et al., 2009; Kamachi et al., 2001). However, roles for Sox2 in other components of the visual system, in particular the dLGN, are still unexplored. So far, Sox2 function has been prominently demonstrated in stem cells (embryonic, neural) (Arnold et al., 2011; Avilion et al., 2003; Favaro et al., 2009; Pevny and Nicolis, 2010; Bertolini et al., 2019); instead, neuronal differentiation implies Sox2 extinction, with rare exceptions (Graham et al., 2003; Lee et al., 2014).

Here, we report that SOX2 is highly expressed in postmitotic, fully differentiated projection neurons of the dLGN. We find that its thalamic-specific ablation in these neurons impairs the development of dLGN, in particular its connectivity with the retina and the visual cortex, and we identify specific SOX2 downstream target genes that likely contribute to these defects.

[1]Department of Biotechnology and Biosciences, University of Milano-Bicocca, piazza della Scienza 2, 20126 Milano, Italy

[2]Clinical and Experimental Epileptology Unit, Fondazione I.R.C.C.S. Istituto Neurologico "Carlo Besta", c/o AMADEOLAB, via Amadeo 42, 20133 Milano, Italy

[3]Centro de Biología Molecular Severo Ochoa, Consejo Superior de Investigaciones Científicas - Universidad Autónoma de Madrid and CIBER de Enfermedades Raras (CIBERER), ISCIII Madrid, Madrid, Spain

[4]The Francis Crick Institute, Midland Road, London NW 1AT, UK

[5]Université Côte d'Azur, CNRS, Inserm, iBV, Nice, France

[6]Lead Contact

*Correspondence: silvia.nicolis@unimib.it

https://doi.org/10.1016/j.isci.2019.04.030

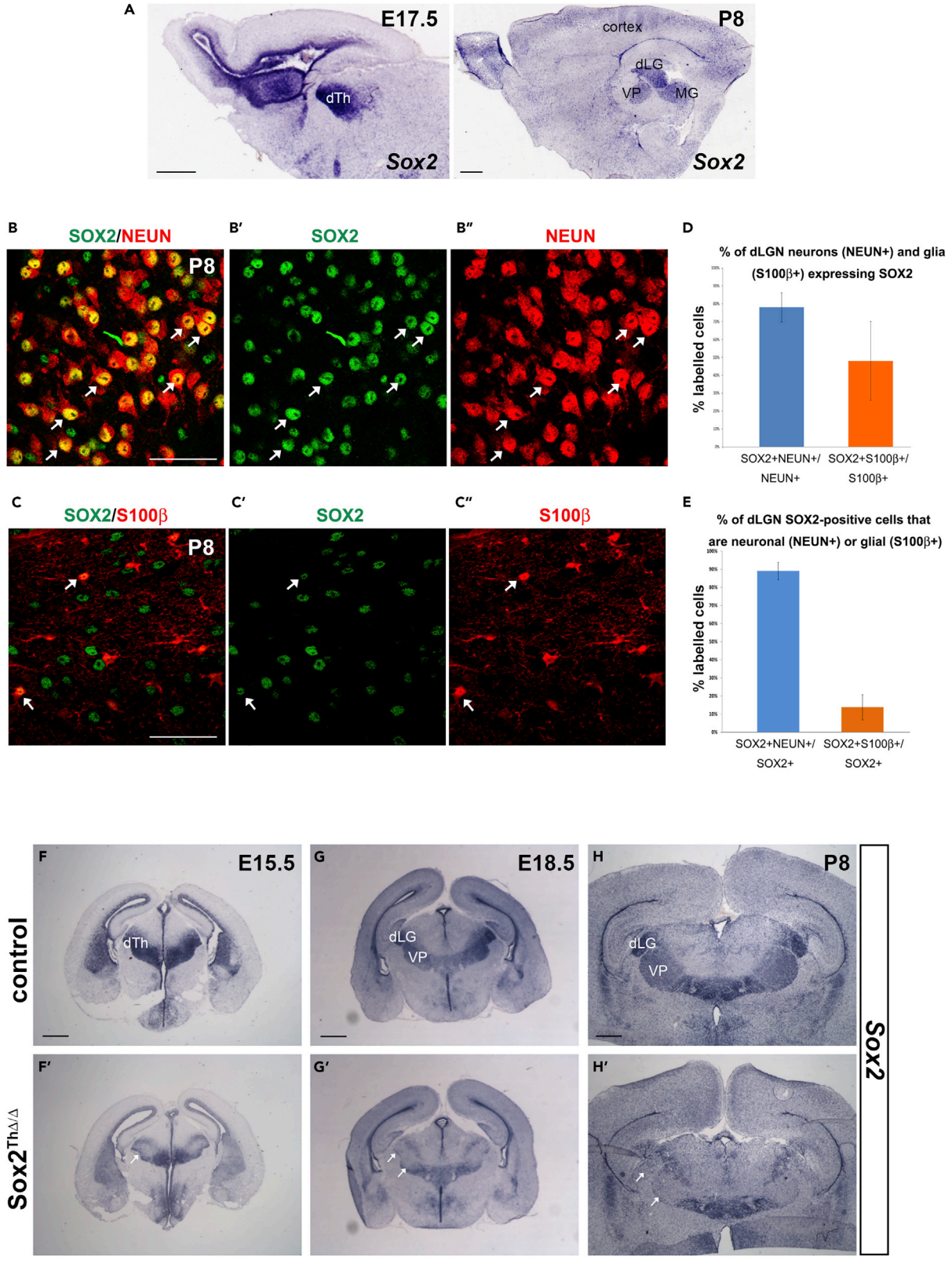
A
E17.5
dTh
Sox2
cortex
P8
dLG
VP
MG
Sox2
B
SOX2/NEUN
P8
B′
SOX2
B″
NEUN
C
SOX2/S100β
P8
C′
SOX2
C″
S100β
D
% of dLGN neurons (NEUN+) and glia (S100β+) expressing SOX2
% labelled cells
SOX2+NEUN+/ NEUN+
SOX2+S100β+/ S100β+
E
% of dLGN SOX2-positive cells that are neuronal (NEUN+) or glial (S100β+)
% labelled cells
SOX2+NEUN+/ SOX2+
SOX2+S100β+/ SOX2+
control
Sox2ThΔ/Δ
F
E15.5
dTh
G
E18.5
dLG
VP
H
P8
dLG
VP
F′
G′
H′
Sox2

Figure 1. Sox2 Thalamic Expression and Its Thalamic Ablation

(A) *In situ* hybridization with a *Sox2* probe on sagittal sections of mouse brain at E17.5 and P8. *Sox2* thalamic expression in the dorsal thalamus (dTh) at E17.5 and in the thalamic nuclei MG, dLG, and VP at P8 can be observed.

(B–C″) Immunofluorescence on coronal sections of dLG of mouse brain at P8 with anti-SOX2 (green) and anti-NEUN (red), a neuronal marker, antibodies in (B–B″) and with anti-SOX2 (green) and anti-S100β (red), an astroglial marker, antibodies in (C–C″). Arrows indicate cells co-expressing SOX2 and NEUN (B–B″) or SOX2 and S100β (C–C″) (n = 3).

(D) Quantification of the number of cells in the dLG at P8 positive for both SOX2 and NEUN out of the total number of NEUN-positive cells (blue) and of the number of cells positive for both SOX2 and S100β out of the total number of S100β-positive cells (orange). Around 80% of NEUN-positive neurons express SOX2. Data are represented as mean ± standard deviation.

(E) Quantification of the number of SOX2-and NEUN-positive cells in the dLG at P8 out of the total number of SOX2-positive cells (blue) and of the number of SOX2-and S100β-positive cells out of the total number of SOX2-positive cells (orange). Around 90% of SOX2-positive cells are neurons (n = 3). Data are represented as mean ± standard deviation.

(F–H′) *In situ* hybridization with a *Sox2* probe on coronal sections of mouse brains at E15.5 (F and F′), E18.5 (G and G′), and P8 (H and H′) of Sox2 thalamic mutants $Sox2^{Th\Delta/\Delta}$ (F′, G′, and H′) and control littermates ($Sox2^{Th\Delta/+}$ or $Sox2^{Th+/+}$) (F, G, and H). A clear ablation of *Sox2* expression in the dorsal thalamus of Sox2 thalamic mutants (arrows) is observed at all stages compared with controls (E15.5 control n = 2, mutant n = 2; E18.5 control n = 3, mutant n = 2; P8 control n = 2, mutant n = 2). Scale bars, 600 μm in (A and F–H′) and 50 μm in (B–C″).

dTh, dorsal thalamus; MG, medial geniculate nucleus; dLG, dorso-lateral geniculate nucleus; VP, ventro-posterior nucleus.

RESULTS

Sox2 Is Expressed in Thalamic Projection Neurons

We first investigated Sox2 expression in the thalamus by *in situ* hybridization (ISH) and immunofluorescence (IF) (Figure 1). ISH detects high Sox2 expression in the dorsal thalamus at perinatal stages (embryonic day [E] 17.5), and in the sensory thalamic nuclei, including the dLGN, at postnatal stages (P8) (Figure 1A). At these late stages, thalamic cells consist of differentiated neurons and glia (Gezelius and Lopez-Bendito, 2017). Indeed, IF on the postnatal dLGN shows that the vast majority of cells positive for NEUN (a general marker of differentiated neurons) are strongly positive for SOX2 (Figures 1B and 1D). A proportion of glial cells (about 50%), marked by S100β, are also weakly SOX2 positive (Figures 1C and 1D). Overall, most (89%) SOX2-positive dLGN cells are represented by neurons (Figure 1E). On the other hand, interneurons, marked by GAD67, are SOX2 negative (Figure S1A), indicating that, within neurons, SOX2 activity is mainly restricted to glutamatergic (projection) neurons. The majority of oligodendrocytes, marked by OLIG2, are SOX2 negative with some minor exceptions (Figure S1B).

Sox2 Deletion in the Developing Thalamus Leads to Reduced dLGN Size and Reduced Retinal Afferents to the dLGN

To delete Sox2 in the thalamus, we used a $Sox2^{flox}$ allele that we had previously generated (Favaro et al., 2009), in combination with a RORα-Cre transgene, active from E14.5, when thalamic neurons are already postmitotic (Chou et al., 2013). Sox2-efficient ablation was observed by ISH, already at E15.5 in the dorsal thalamus (Figures 1F and 1F′), and, subsequently (E18.5, P8; Figures 1G–1H′), in the dLGN and in the adjacent somatosensory thalamic nucleus (ventro-posterior nucleus [VPN]) (Chou et al., 2013). Sox2 thalamic mutants are termed $Sox2^{Th\Delta/\Delta}$ hereafter. IF shows that SOX2 is efficiently ablated from neurons, although it persists in at least some glia (Figures S1C and S1D).

To determine if Sox2 thalamic ablation results in defects in normal development of thalamic nuclei, in particular of the visual thalamic nucleus (dLGN), we analyzed by ISH the expression of the transcription factor Lef1, present in the dLGN, but almost absent in the adjacent ventro-lateral geniculate nucleus (vLGN) (Figures 2A–2D′). At the end of gestation (E18.5), the mutant dLGN did not overtly differ in size from controls (Figures 2A and 2A′); however, in postnatal development, the mutant dLGN failed to increase in size, contrary to controls, as seen by Lef1 ISH (Figures 2B–2D′) and Nissl staining (Figures 2E and 2E′).

In normal development of visual system connectivity, retinal axons outgrow toward the dLGN, and establish neuron-to-neuron connections with the cell bodies of dLGN neurons. The dLGN provides molecular signals that guide and precisely pattern the outgrowth of incoming retinal axon terminals to form appropriately localized connections to the dLGN during the perinatal and early postnatal periods; retinal afferents are, in turn, the source of important trophic signals, that allow the dLGN to complete its development and growth in early postnatal life (El-Danaf et al., 2015; Guido, 2018). IF with antibodies against the vesicular glutamate transporter 2 (VGLUT2) detects glutamatergic neuronal afferents from the retina, ensheathing and defining the dLGN. VGLUT2 IF showed an overall reduced area of the dLGN signal in the mutant at postnatal stages, confirming a reduced size (Figures 2F and 2F′), a result that is also observed

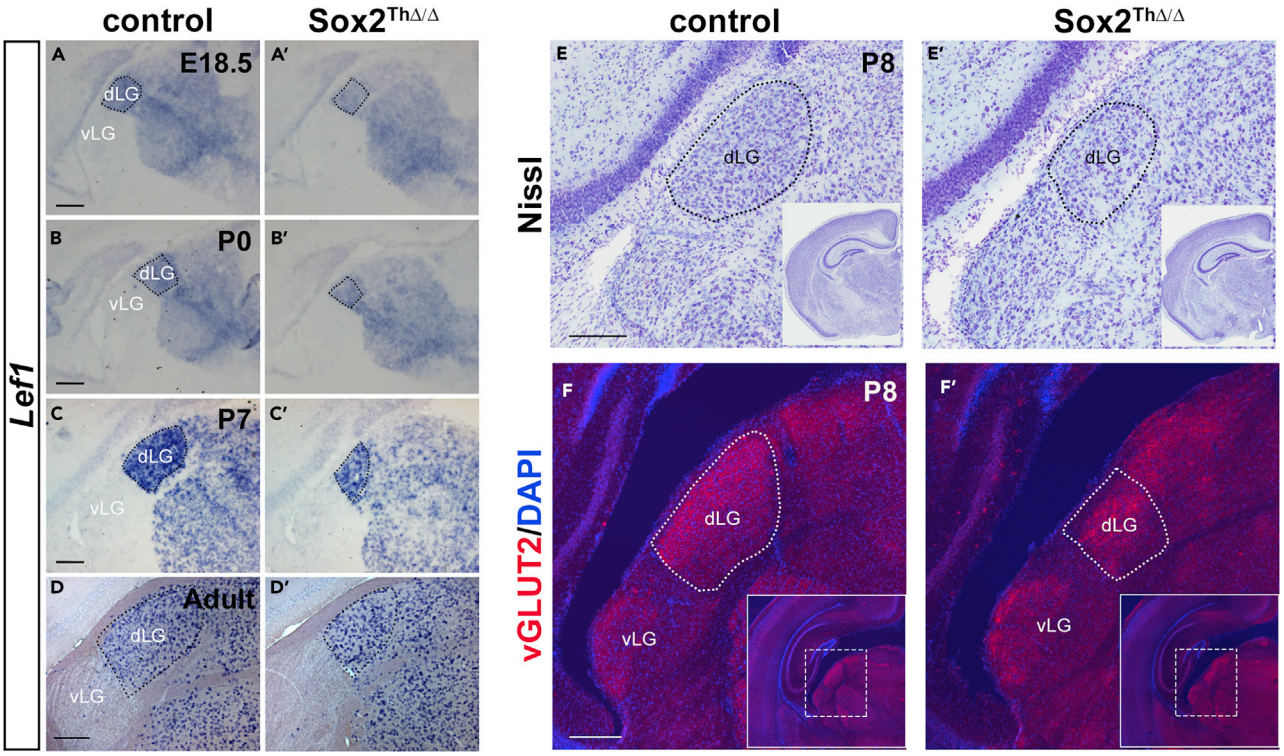
control
Sox2ThΔ/Δ
Lef1
A
E18.5
dLG
vLG
A′
B
P0
B′
C
P7
C′
D
Adult
D′
control
Sox2ThΔ/Δ
Nissl
E
P8
E′
vGLUT2/DAPI
F
F′

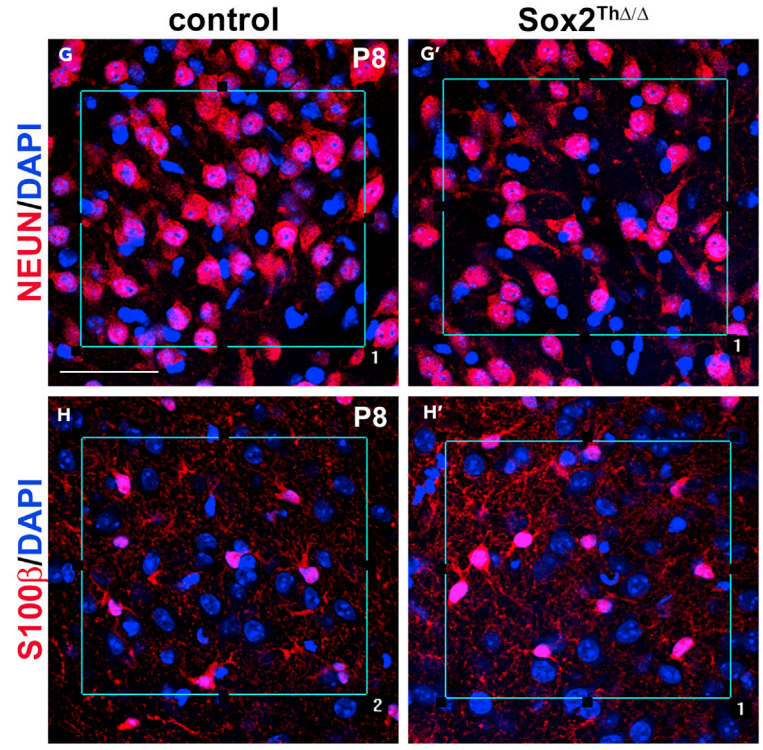
control
Sox2ThΔ/Δ
NEUN/DAPI
G
P8
G′
S100β/DAPI
H
H′

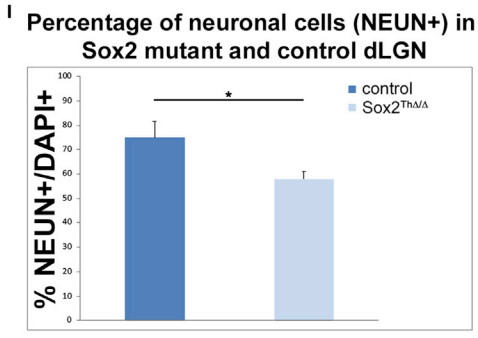
I
Percentage of neuronal cells (NEUN+) in Sox2 mutant and control dLGN
% NEUN+/DAPI+
control
Sox2ThΔ/Δ
*

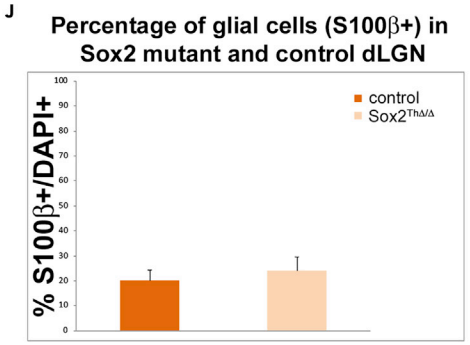
J
Percentage of glial cells (S100β+) in Sox2 mutant and control dLGN
% S100β+/DAPI+
control
Sox2ThΔ/Δ

Figure 2. The dLG Nucleus Is Reduced in Size in Sox2 Thalamic Mutants

(A–D′) *In situ* hybridization with a *Lef1* probe on coronal sections of mouse brains at E18.5 (A and A′), P0 (B and B′), P7 (C and C′), and adults (D and D′) of Sox2 thalamic mutants (A′, B′, C′, and D′) and control littermates (A, B, C, and D). The dLG, marked by *Lef1* expression, is reduced in size in the mutants starting at P0 (E18.5 control n = 6, mutant n = 6; P0 control n = 4, mutant n = 4; P7 control n = 5, mutant n = 3; adult control n = 2, mutant n = 2).

(E and E′) Nissl staining of coronal sections of mouse brains at P8 of Sox2 thalamic mutants (E′) and control littermates (E). The dLG is reduced in size in mutants compared with controls (control n = 2, mutant n = 2).

(F and F′) Immunofluorescence with an anti-vGLUT2 antibody (in red) on coronal sections of dorsal thalamus at P8 of Sox2 thalamic mutants (F′) and control littermates (F). Nuclei are marked by DAPI (blue). The mutant dLG marked by VGlut2-expressing retinal fibers appears reduced in size compared with controls (control n = 4, mutant n = 2). Dotted lines outline the dLG.

(G–H′) Immunofluorescence on coronal sections of mouse dLG at P8 of Sox2 thalamic mutants (G′ and H′) and control littermates (G and H) with antibodies anti-NEUN (a neuronal marker, in red) (G and G′) and anti-S100β (an astroglial marker, in red) (H and H′). Nuclei are marked by DAPI (blue) (control n = 3, mutant n = 3).

(I) Quantification of the percentage of NEUN-positive cells out of DAPI-positive cells in control and mutant dLG nuclei.

(J) Quantification of the percentage of S100β-positive cells out of total DAPI-positive cells in control and mutant dLG nuclei. A slight reduction of NEUN-positive neurons in the mutant dLG is observed. Error bars represent the standard deviation, * denotes a statistically significant difference $p < 0.05$ ($p = 0.01308$). Scale bars, 200 μm in (A–F′) and 50 μm in (G–H′). dLG, dorso-lateral geniculate nucleus; vLG, ventro-lateral geniculate nucleus.

at P16 and in adults (Figures S2A–S2B′). Interestingly, the area covered by the incoming VGlut2-positive fibers reaching the vLGN appeared slightly expanded (Figures 2F and S2A–S2B′). In addition, in both P16 and adult mutants, the signal was less uniformly distributed than in controls and more concentrated on the dorsal side of the dLGN (Figures S2A–S2B′).

A postnatally reduced size of the mutant dLGN (but not vLGN) was further confirmed by area measurements on DAPI-stained sections, in which retinal afferents had been stained with cholera toxin (Figures S2C–S2E; cholera toxin labeling will be described in Figure 3).

In the mutant dLGN (P8), the frequency of neurons (NEUN-positive cells) was reduced (by 18%), whereas that of glia (S100β-positive) was not significantly altered (Figures 2G–2J).

Taken together, these results highlight that the mutant dLGN does not grow, postnatally, contrary to the control dLGN, and that, concomitantly, a reduction of retinal afferents reaching the mutant dLGN is observed.

Retino-Thalamic Projections Are Abnormally Distributed in Sox2 Thalamic Mutants

In normal development, naso-temporal retinal projections from each eye cross on the brain midline (optic chiasm) to reach a specific region of the contralateral dLGN, whereas a minority of the fibers from the ventro-temporal crescent of the retina do not cross and project onto the ipsilateral dLGN. dLGN regions receiving the contra- or ipsilateral fibers have well-defined, complementary, mutually exclusive shapes, that can be visualized by separately marking the retinal fibers originating from the right and left eyes with cholera toxin subunit B labeled with different fluorochromes (Figure 3; see drawing in Figure 3K). We labeled retinal afferents at three time points (P0, P7, P21), defining successive steps of afferents arrival to the dLGN, and segregation within it, and analyzed the projections to the thalamus 1–3 days later (P1, P9 and P24, Figures 3A–3H″). In mutants, retinal afferents to the dLGN are reduced already at the earliest time point (P1, Figures 3A and 3B), particularly in the medial dLGN region (arrows). Of note, the size of the dLGN is still comparable in mutants and control at this early stage. At later stages (P9, P24), in controls, contra (green)- and ipsilateral (red) afferents complete their segregation to different regions of the dLGN, as expected (Figures 3C and 3E). In mutants, segregation occurs, but the pattern of ipsi- and contralateral afferent fibers appears abnormal: ipsilateral (red) fibers show a different distribution (compare the mutants in Figure 3D, and particularly Figures 3G and 3H, versus controls in Figures 3C, 3E, and 3F, respectively); contralateral (green) fibers also look abnormal, with a somewhat fragmented, "clumpy" fiber distribution, in particular the most anterior (left) sections (Figure 3D compared with Figure 3C, Figure 3G compared with Figure 3E; arrowheads in Figures 3D and 3G point to "clumps," i.e., local dishomogeneities, in mutant). In addition, at both early (P1) and later (P9, P24) stages, in mutants, the fraction of retinal afferents reaching the vLGN (measured as the green area in the vLGN) is proportionally higher than that reaching the dLGN when compared with controls, suggesting afferents misrouting (Figure 3D versus Figure 3C, and Figures 3G and 3H versus Figures 3E and 3F; see Figures 3I and 3J for quantifications). Finally, in mutants, an abnormally increased fraction of contralateral fibers was also apparent in the intermediate lateral geniculate nucleus (iLGN) (Figure 3G versus 3E), and, within the vLGN, some overlap between contra- and ipsilateral

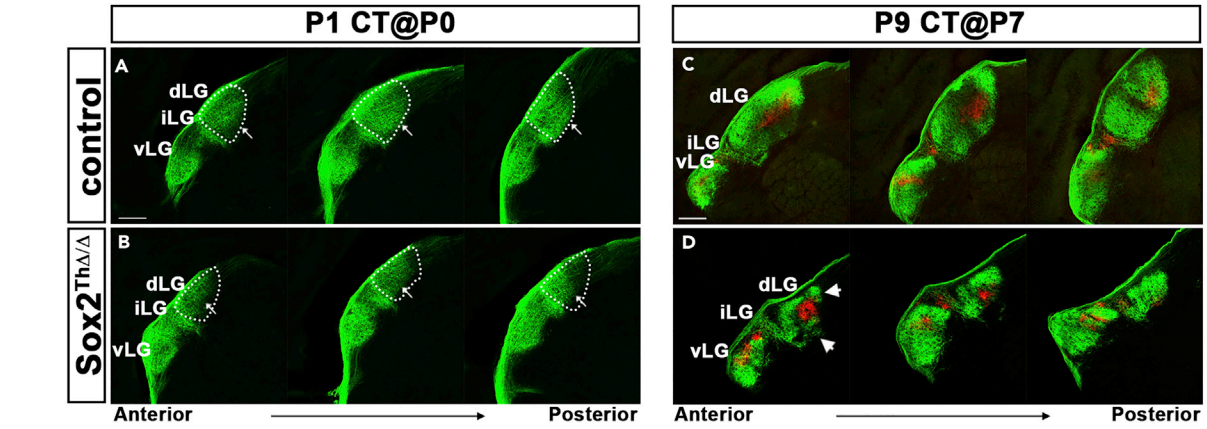
P1 CT@P0
P9 CT@P7
control
Sox2ThΔ/Δ
A
B
C
D
dLG
iLG
vLG
Anterior
Posterior

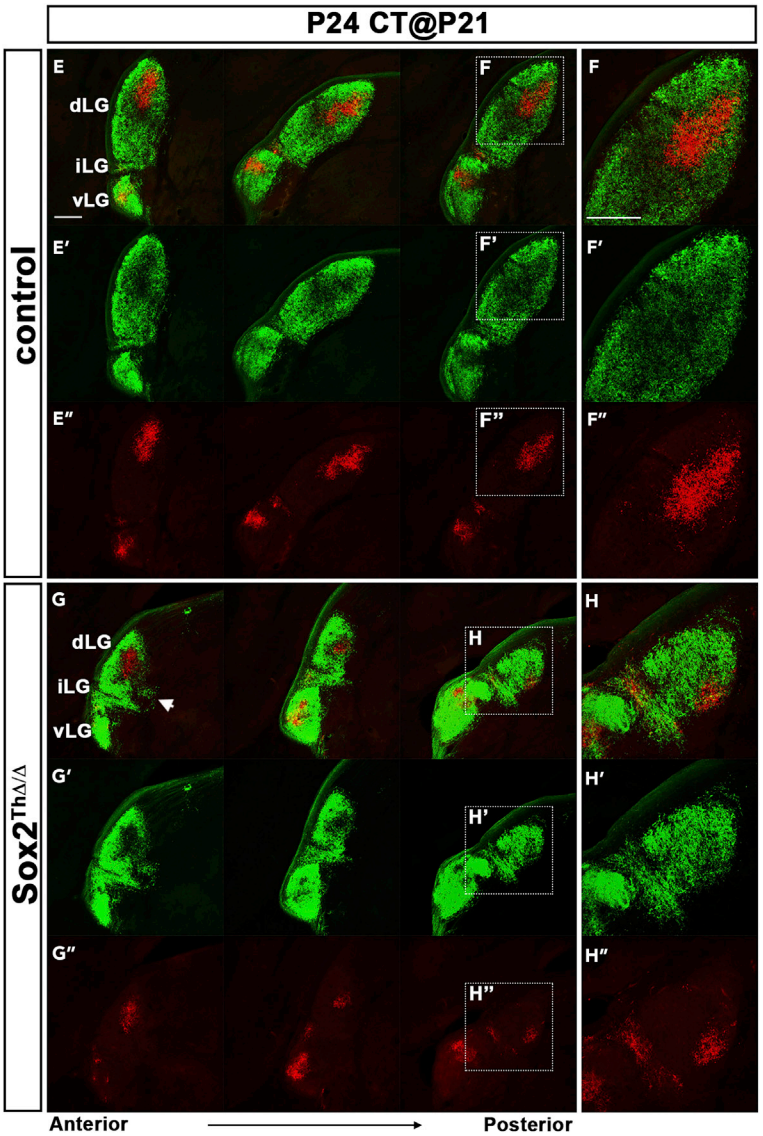
P24 CT@P21
control
Sox2ThΔ/Δ
E
E′
E″
F
F′
F″
G
G′
G″
H
H′
H″
dLG
iLG
vLG
Anterior
Posterior

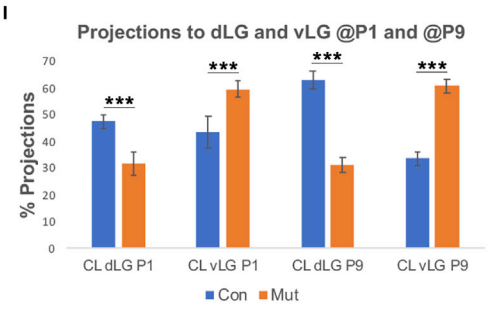
I
Projections to dLG and vLG @P1 and @P9
% Projections
CL dLG P1
CL vLG P1
CL dLG P9
CL vLG P9
Con
Mut

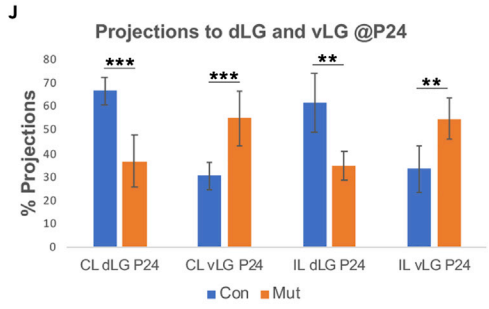
J
Projections to dLG and vLG @P24
% Projections
CL dLG P24
CL vLG P24
IL dLG P24
IL vLG P24
Con
Mut

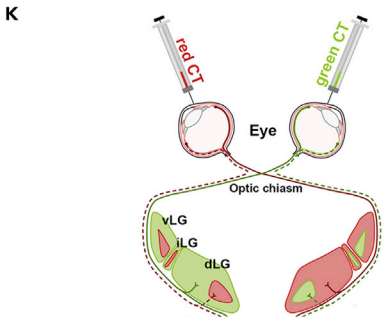
K
red CT
green CT
Eye
Optic chiasm
vLG
iLG
dLG

Figure 3. Defects in Retinal Projections to the dLG Are Found in Sox2 Thalamic Mutants

(A–H″ and K) Choleratoxin (CT) subunit B -Alexa 488 (green) and CT subunit B-Alexa 594 (red) were injected, respectively, in the right and left eyes, and contralateral (green) and ipsilateral (red) axons to the left dLG and vLG are shown (see scheme of injection in K modified from Seabrook et al., 2017). Series of coronal sections of the dLG from anterior (left) to posterior (right) of representative Sox2 thalamic mutants (B, D, G, and H) and littermate controls (A, C, E, and F) are shown. (A and B) CT was injected at P0, and brains were analyzed at P1. Less retinal axons are observed in the mutant dLG. Arrows mark the medial border of contralateral projections. (C and D) CT was injected at P7, and brains were analyzed at P9. Retinal axons arrive to a smaller dLG in mutants, and projections are often fragmented (arrowheads). (E–H″) CT was injected at P21, and brains were analyzed at P24. Retinal projections in mutants arrive to a smaller dLG and are sometimes fragmented (arrowheads) compared with controls (P1 control n = 4, mutant n = 4; P9 control n = 3, mutant n = 4; P24 control n = 3, mutant n = 3).

(I) Quantification of the percentage of contralateral (CL) retinal axons that reach the dLG or vLG in mutants and controls at P1 and P9 (***$p < 0.005$, unpaired Student's t test).

(J) Quantification of the percentage of retinal axons, contralateral (CL) or ipsilateral (IL), that reach the dLG or vLG in mutants and controls at P24 (P1 control n = 4, mutant n = 3; P9 control n = 2, mutant n = 4; P24 control n = 3, mutant n = 3). Error bars represent standard deviation; * denotes a statistically significant difference with unpaired Student's t test, **$p < 0.01$, ***$p < 0.005$. Scale bars, 200 μm. dLG, dorso-lateral geniculate nucleus; iLG, intermediate lateral geniculate nucleus; vLG, ventro-lateral geniculate nucleus.

projections was visible, possibly as a result of the excess fibers projecting to the vLGN in mutants (see above; Figure 3G compared with Figure 3E).

We also traced the retinal axons reaching the dLGN through 1,1′-dioctadecyl-3,3,3′,3′-tetramethylindocarbocyanine perchlorate (DiI) labeling in early postnatal life (at P0, and P5) (Figures S2F–S2G′). In thalamic Sox2 mutants, an overall reduction of retinal afferents reaching the dLGN is seen already at P0, and, more markedly, at P5 (Figures S2F–S2G′), matching the abnormality observed in the mutant by cholera toxin labeling.

Of note, the thalamic defects did not result in gross alterations of the adult retina or in changes of the number and distribution of the retinal ganglion cells (RGC; Figures S2H and S2I), indicating that, in spite of abnormal targeting, RGC viability is preserved.

Overall, these data indicate a role for Sox2 within dLGN cells, in the generation of appropriate connections of retinal afferents to the thalamus, suggesting a possible role for Sox2 in regulating guidance cues in the thalamus.

Thalamo-Cortical Connections and Normal Postnatal Patterning of the Cerebral Cortex Are Perturbed in Sox2 Thalamic Mutants

To directly investigate thalamo-cortical connections in mutants, we performed immunohistochemistry (on cortical flat mounts, scheme in Figure 4A, and telencephalon coronal sections) with antibodies against VGlut2 (Figures 4B and 4D), the serotonin transporter (SERT) (Figures 4C and 4E), and serotonin (5-hydroxytryptamine [5-HT[) (Figure 4F), all marking the developing thalamo-cortical axons (TCA) in the young postnatal brain (Chou et al., 2013; Lebrand et al., 1996). With all three antibodies, a reduction of the staining was observed in the visual cortex (V1) in $Sox2^{Th\Delta/\Delta}$ mutants (Figures 4B′–4F′, compared with Figures 4B–4F), indicating that TCA originating from mutant dLGN are strongly abnormal.

The correct development of TCA, projecting from the dLGN to the visual cortex, is essential for the development of the cortical visual areas, in particular for the diversification of the primary visual area (V1) and the adjacent higher-order visual areas (V^{HO}) (Chou et al., 2013). In the normal postnatal brain (P7), the *Lmo4* gene is expressed in V^{HO}, but not in the adjacent V1, with a clear boundary between positive and negative regions; in the mutant, however, this boundary is not well defined, and expression in V1 is more pronounced and more similar to that in V^{HO} (Figures 4G and 4G′). We also obtained similar results with two different markers, *Bhlhb5*, normally expressed in the V1, but less so in the V_{H0} area (Figures 4H and 4H′), and *Rorβ* (not shown). The observed cortical defect is reminiscent of alterations previously found in Nr2f1 (COUP-TF1) thalamic mutants obtained by RORα-Cre-mediated deletion of the *Nr2f1* gene, encoding a transcription factor important for dLGN neurons development. In these mutants, the cortical defects are thought to be secondary to defective TCA connections of the dLGN to the visual cortex (Chou et al., 2013).

Overall, the detection of a cortical patterning defect in our thalamic mutant, together with the abnormalities of the incoming thalamic connections (as indicated by the reduced VGlut2 staining), indicates a defect in the development of TCA, affecting their ability to correctly pattern the postnatal cortex.

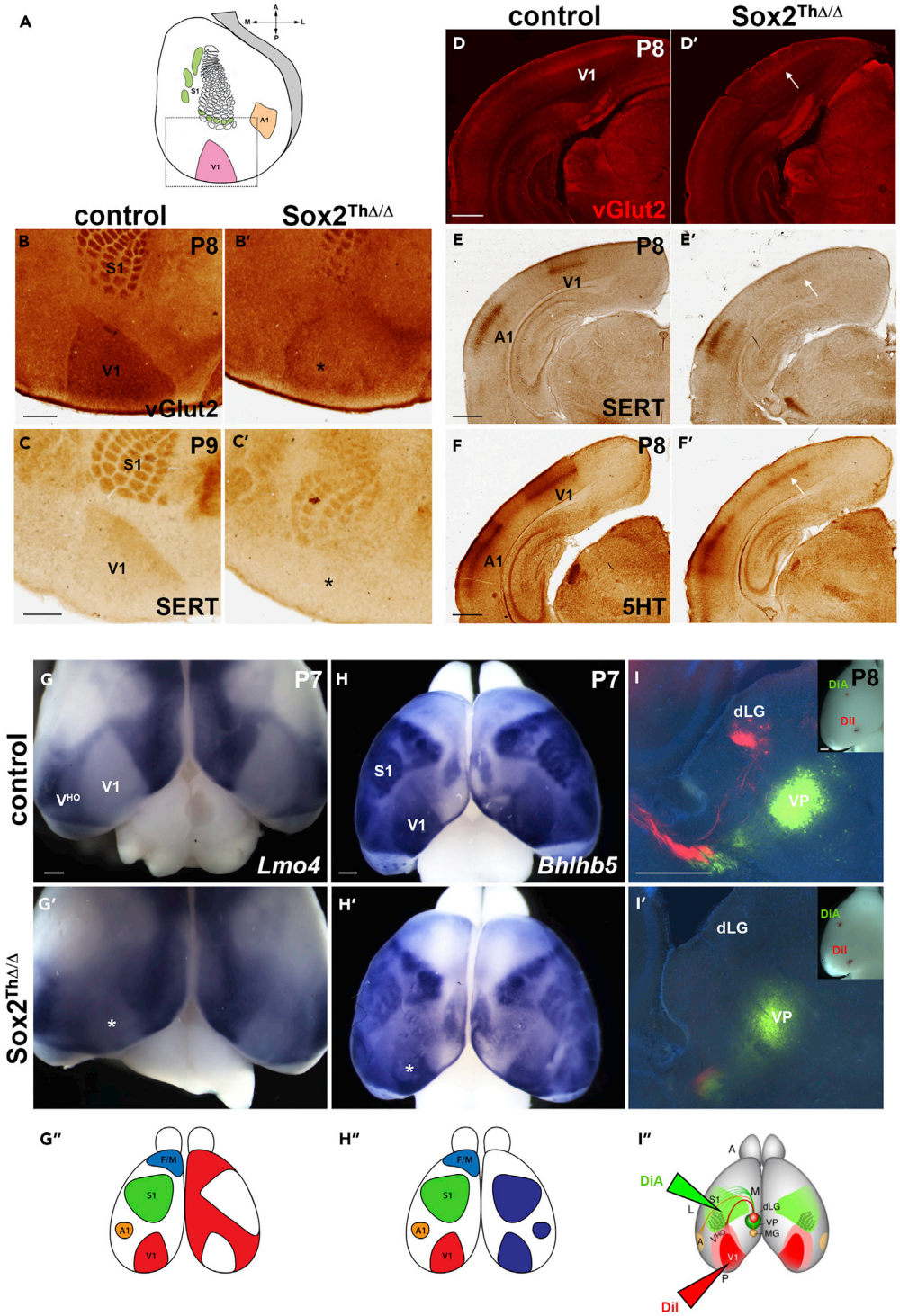

Figure 4. Thalamo-Cortical Connectivity and Cortical Patterning Are Abnormal in Sox2 Thalamic Mutants

(A) Representation of a cortical flat mount.

(B–C′) Immunohistochemistry on tangential sections of cortical flat mounts at P8 of Sox2 thalamic mutants (B′ and C′) and controls (B and C) with VGlut2 (B and B′) and serotonin transporter (SERT) (C and C′) both expressed by thalamic projections to the cortex. Staining in the mutant visual cortex is reduced (*) with both markers compared with controls (VGlut2 control n = 16, mutant n = 7; SERT control n = 6, mutant n = 3).

Figure 4. *Continued*

(D and D′) Immunofluorescence with VGlut2 on coronal sections of mouse brains at P8. VGlut2-positive thalamo-cortical projections to V1 are reduced in Sox2 mutants (D′) compared with controls (D) (white arrow) (control n = 4, mutant n = 2).

(E–F′) Immunohistochemistry on coronal sections of mouse brains at P8 of Sox2 thalamic mutants (E′ and F′) and controls (E and F) with SERT (E and E′) and serotonin (5HT) (F and F′). Staining in the mutant V1 is reduced with both markers (white arrows) (SERT control n = 4, mutant n = 2; 5-HT control n = 5, mutant n = 3).

(G–H″) (G–H′) Whole-mount *in situ* hybridization for the cortical markers *Lmo4* (G and G′) and *Bhlhb5* (H and H′) (schematic expression pattern in G″ and H″) on Sox2 thalamic mutants and littermate controls. The mutant visual area (V1) is not clearly distinguished from the neighboring higher-order visual areas (V^{HO}) compared with control V1 (see *) (*Lmo4* control n = 6, mutant n = 3; *Bhlhb5* control n = 11, mutant n = 5).

(I–I″) (I and I′) Coronal sections at P8 after insertion of DiI crystals (scheme in I″ modified from Chou et al., 2013) in the primary visual cortex (V1) (red) and DiA in the somatosensory cortex (S1) (green) showing axons projecting to the dLG in controls and not in Sox2 thalamic mutants (control hemispheres n = 28, mutant hemispheres n = 15). Scale bars, 600 μm.

V1, primary visual area; V^{HO}, higher-order visual area; S1, primary somatosensory area; A1, primary auditory area; dLG, dorso-lateral geniculate nucleus; VP, ventro-posterior nucleus; MG, medial geniculate nucleus; F/M, motor cortex.

The thalamus is also the target of cortico-thalamic axon afferents (CTA) (Garel and Lopez-Bendito, 2014). We injected DiI (red) and 4-(4-(dihexadecylamino)styryl)-N-methylpyridinium iodide (DiA) (green) in the visual and somatosensory cortex, respectively (scheme in Figure 4I″); these compounds diffuse along the neuronal membranes, allowing visualization of neuronal projections. Labeling of visual cortex with DiI showed that development of CTA to the dLGN was compromised in $Sox2^{Th\Delta/\Delta}$ mutants, whereas the connections between the somatosensory cortex and the VPN were comparatively less affected (Figures 4I–4I″).

Overall, our observations show that Sox2 ablation affects TCA development, and, secondarily, cortical patterning and CTA development.

Specific Genes Important for dLGN Development Are Downregulated in the Mutant dLGN

To identify Sox2 target genes whose deregulation in Sox2 mutants might be responsible for the observed defects of connectivity, we studied the expression of candidate genes known to play key roles in dLGN development, by ISH and immunohistochemistry (Figures 5 and S3). In the dLGN, (and VPN), Sox2 was co-expressed with Nr2f1 (data not shown); however, no important reduction was detected, in mutants, in the expression of *Nr2f1* by ISH (Figures 5B and 5B′) or immunohistochemistry (at E18.5 and P8, not shown). Also, no change was found in the expression of other genes normally active, and important, in or for the dLGN, tested at E18.5 or at E15.5: *Zic4* (Horng et al., 2009), *NtnG1*, *Sema6A* (Gezelius and Lopez-Bendito, 2017; Little et al., 2009), *Gbx2* (Miyashita-Lin et al., 1999; Sur and Rubenstein, 2005), *Sox11*, *Klf6*, *Zic1*, and *Ntn1* (Braisted et al., 2000) (Figures 5C–5E′, S3B–S3D′, and S3F–S3H′). This indicates that a "general" dLGN gene expression program was retained in mutant dLGN.

However, in the mutant dLGN we observed a strong reduction in the expression of *ephrin-A5* (encoded by the *Efna5* gene) by ISH E18.5, i.e., before the visible patterning defect, and postnatally (P7) (Figures 5F–5H″). Of note, some reduction was consistently observed also in heterozygotes (Figures 5G′ and 5H′, compared with Figures 5G and 5H).

Ephrin-A5 is a signaling molecule involved in axon guidance in the developing brain (Kania and Klein, 2016) and is expressed, in the normal dLGN, in a gradient. Germline KO studies showed that, in the absence of Efna5, 2, and 3, the establishment of the correct pattern of contra- and ipsilateral retina-dLGN projections is severely disrupted (Huberman et al., 2005; Pfeiffenberger et al., 2005; Vanderhaeghen et al., 2000); these previous results suggest that Efna5 downregulation in Sox2 mutants may significantly contribute to the observed defective patterning of retinal afferents. Interestingly, SOX2 chromatin immunoprecipitation (ChIP-seq) detects two SOX2-bound regions in the *Efna5* gene in neural stem or progenitor cells, located in the first intron (Figure 5I). We cloned each of the two DNA regions encompassing the SOX2 peaks upstream of a minimal promoter and a luciferase reporter gene (Figure 5J) and co-transfected the constructs with increasing amounts of a SOX2 expression vector (Ferri et al., 2013; Mariani et al., 2012; Panaliappan et al., 2018) into neural (Neuro-2a) cells (Figure 5K). The most upstream peak (5′ peak) did not show any response over the SOX2 amounts tested; the 3′ peak, however, showed a strong dose-dependent transactivation of the luciferase reporter, to an extent similar to that previously observed with the promoter of the Nkx2.1 gene, a previously identified SOX2 target (Ferri et al., 2013) (Figure 5K). These observations indicate the presence of a SOX2-responsive regulatory region (putative enhancer) within the Efna5 gene.

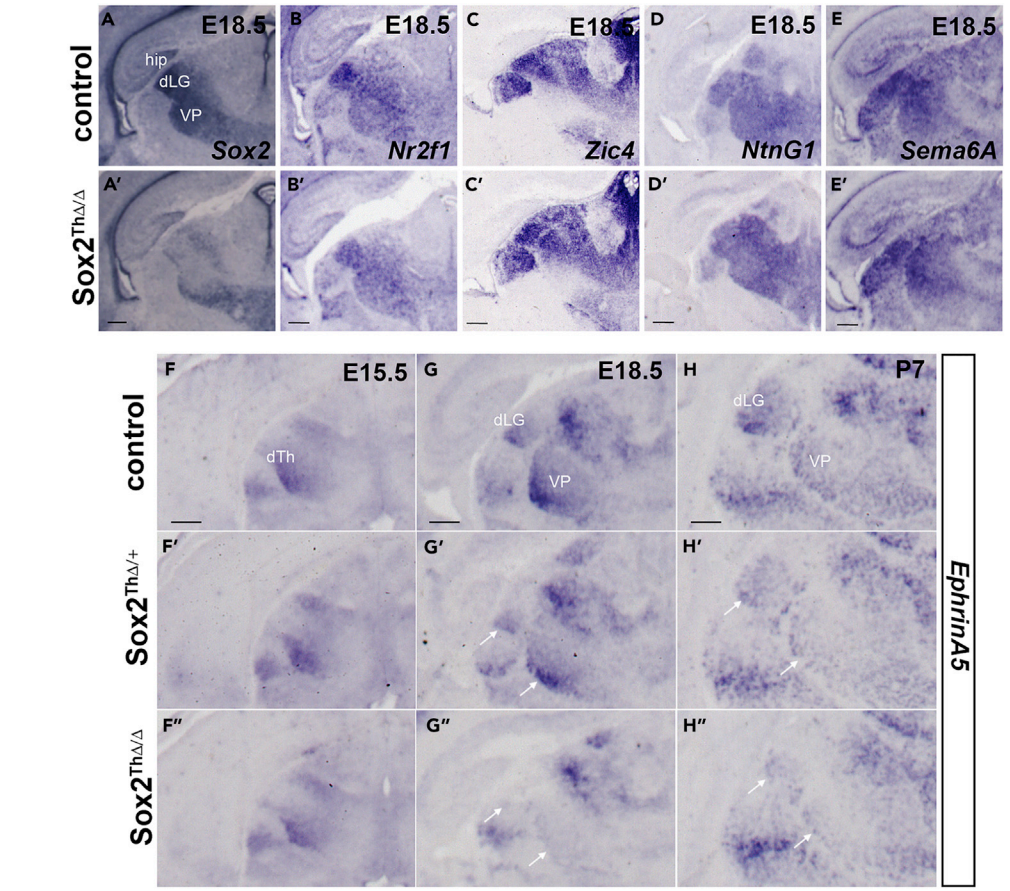
A
E18.5
hip
dLG
VP
Sox2
B
E18.5
Nr2f1
C
E18.5
Zic4
D
E18.5
NtnG1
E
E18.5
Sema6A
control
A′
B′
C′
D′
E′
Sox2ThΔ/Δ
F
E15.5
dTh
G
E18.5
dLG
VP
H
P7
dLG
VP
control
F′
G′
H′
Sox2ThΔ/+
F″
G″
H″
Sox2ThΔ/Δ
EphrinA5

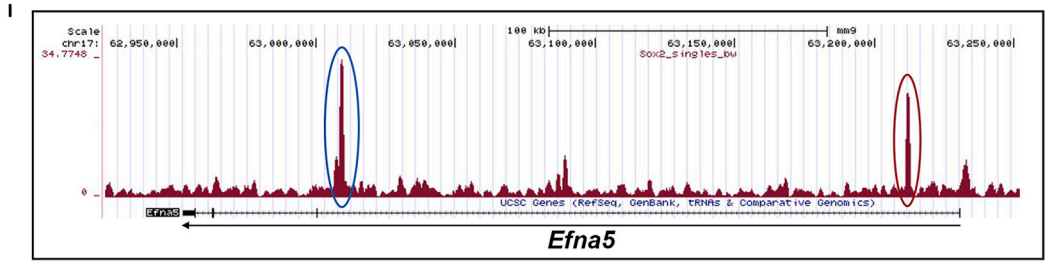
I
Scale
chr17:
34.7748
62,950,000
63,000,000
63,050,000
100 kb
63,100,000
63,150,000
Sox2_singles_bw
mm9
63,200,000
63,250,000
UCSC Genes (RefSeq, GenBank, tRNAs & Comparative Genomics)
Efna5
Efna5

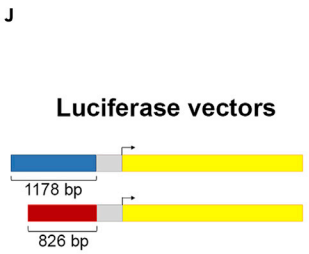
J
Luciferase vectors
1178 bp
826 bp

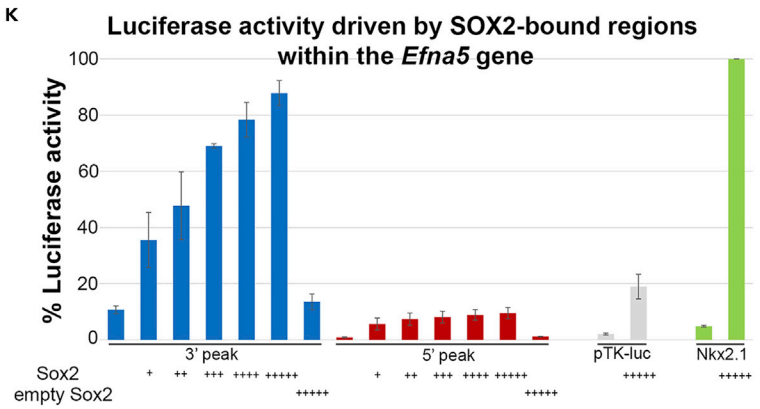
K
Luciferase activity driven by SOX2-bound regions
within the Efna5 gene
% Luciferase activity
100
80
60
40
20
0
3′ peak
5′ peak
pTK-luc
Nkx2.1
Sox2
empty Sox2
+
++
+++
++++
+++++

Figure 5. *Efna5* Expression Is Reduced in the dLG of Sox2 Thalamic Mutants, and a DNA Region within the *Efna5* Locus Is Bound and Activated by SOX2

(A–E′) *In situ* hybridization on coronal sections of mutant (A′, B′, C′, D′, and E′) and control (A, B, C, D, and E) mouse forebrain at E18.5 with *Sox2* (A and A′), *Nr2f1* (B and B′), *Zic4* (C and C′), *Netrin G1* (*NtnG1*; D and D′), and *Semaphorin 6A* (*Sema6A*; E and E′) probes. *Sox2* expression is clearly ablated in the mutant thalamus (A′ compared to A), whereas the expression of the other markers appears unchanged (at least three controls and three mutants were analyzed for each probe).

(F–H″) Time course of *Ephrin-A5* (*Efna5*) expression by *in situ* hybridization on coronal sections of controls, heterozygotes, and homozygote Sox2 thalamic mutant forebrains at E15.5 (F–F″), E18.5 (G–G″), and P7 (H–H″). *Efna5* is specifically downregulated in the dLG and VP of Sox2 homozygote thalamic mutants (white arrows), whereas it remains unchanged in other domains of expression both at E18.5 (G–G″) and P7 (H–H″). A mild *Efna5* downregulation is also observed in Sox2 heterozygotes (G′ and H′) (E15.5 control n = 3, heterozygote n = 3, mutant n = 4; E18.5 control n = 8, heterozygote n = 7, mutant n = 8; P7 control n = 3, heterozygote n = 3, mutant n = 5).

(I) Sox2 ChIP-seq profile across the *Efna5* locus from neurosphere cultures derived from postnatal mouse telencephalon showing two Sox2 peaks (5′, red circle; 3′, blue circle) within the first intron of the *Efna5* gene.

(J) Schematic representation of plasmids containing the 3′ (blue) or 5′ (red) Sox2-bound regions upstream of a minimal promoter (grey) and luciferase reporter gene (yellow).

(K) Co-transfection in Neuro-2a cells of the constructs in (J) with increasing amount of SOX2-expressing vector or with the corresponding empty vector (+, 1:0.06; ++, 1:0.125; +++, 1:0.187; ++++, 1:0.25; +++++, 1:0.5 reporter:transactivator molar ratio). The previously known activation of the Nkx2.1 promoter by the SOX2-expressing vector was used as a positive control of transactivation (Ferri et al., 2013). Results are the mean of three independent transfections, each performed in triplicate. Error bars represent standard deviation. Scale bars, 200 μm. hip, hippocampus; dLG, dorso-lateral geniculate nucleus; VP, ventro-posterior nucleus; dTh, dorsal thalamus.

Further to Efna5 downregulation, we had observed a reduction of serotonin (5-HT), and its transporter SERT in TCA at P8 (see above, Figure 4). As serotonin levels in the first two postnatal weeks have been shown to have a role in regulating thalamo-cortical projections (see below), we investigated in more detail the levels of serotonin, and of components of its pathway, during development, following Sox2 thalamic loss.

5-HT marks the TCA during the time window when they first establish their patterned connections with cortical neurons. 5-HT is not synthesized by thalamic neurons, but is transiently uptaken by TCA via the serotonin transporter SERT (Lebrand et al., 1996); pharmacological manipulation of 5-HT uptake, or knockout of the SERT-encoding gene, perturbs sensory TCA development, particularly to the somatosensory cortex, indicating a developmental function for this transient 5-HT uptake (Chen et al., 2015; Gaspar et al., 2003; Persico et al., 2001). This raised the possibility that an early reduction in 5-HT content within thalamic neurons might, as well, contribute to the observed dLGN TCA development defect in Sox2 mutants. Indeed, we observed a reduction of 5-HT levels in cell bodies and axons in the mutant dLGN (more pronounced in homozygous mutants but also detected in heterozygotes) already at P1 (when the dLGN size is still not importantly reduced in homozygous mutants) (Figures 6A–6A″) and at P8 (Figures 6B–6B″). Furthermore, IF for 5-HT indicated that intracellular 5-HT accumulation is not observed in the mutants at P8 (Figures 6C–6C‴; compare Figures 6C and 6C′, control, showing intracellular perinuclear red 5-HT staining, with Figures 6C″ and 6C‴, mutant, showing strongly reduced intracellular 5-HT). We then investigated the expression of the SERT-encoding gene by ISH at early stages (E18.5), preceding the overtly defective phenotype (Figures 6D–6D″). SERT mRNA signal intensity was reduced in $Sox2^{Th\Delta/\Delta}$ and, to a lesser extent, in heterozygotes, at E18.5 (Figures 6D–6D″) (when the mutant dLGN size is similar to control), and P7 (Figures S3I–S3I″). We also observed, at E18.5, a reduction in the expression of the mRNA encoding the vesicular monoamine transporter 2 (vMAT2) (Figures S3J–S3J″), the transporter that packages 5-HT into synaptic vesicles, protecting it from degradation (Gaspar et al., 2003). These findings indicate that 5-HT metabolism or transport is compromised in Sox2 thalamic mutants, which might plausibly contribute to the abnormal development of thalamo-cortical connectivity, in accordance with previous observations on the somatosensory TCA connections (Persico et al., 2001; Chen et al., 2015; Gaspar et al., 2003). SOX2 ChIP-seq in neural stem or progenitor cells detects low-level SOX2 binding to the promoter region of the SERT-encoding gene Slc6a4 (Figure S4A), whereas in the vMAT2-encoding gene (Slc18a2), three intragenic SOX2-binding peaks are detected (Figure S4B). This suggests that SOX2 might directly participate in the regulation of the vMAT2, and, possibly, the SERT-encoding gene.

Overall, our findings indicate that Sox2 controls, possibly through direct binding, downstream target genes important for dLGN development.

Alterations of the Thalamo-Cortical Connections and of the Patterning of the Cerebral Cortex Are Also Observed in the Somatosensory Axis in Sox2 Thalamic Mutants

In examining the components of the visual system, the focus of the present article (dLGN, visual cortex), we noticed that the ventro-posterior (VP) somatosensory thalamic nucleus and VP thalamo-cortical

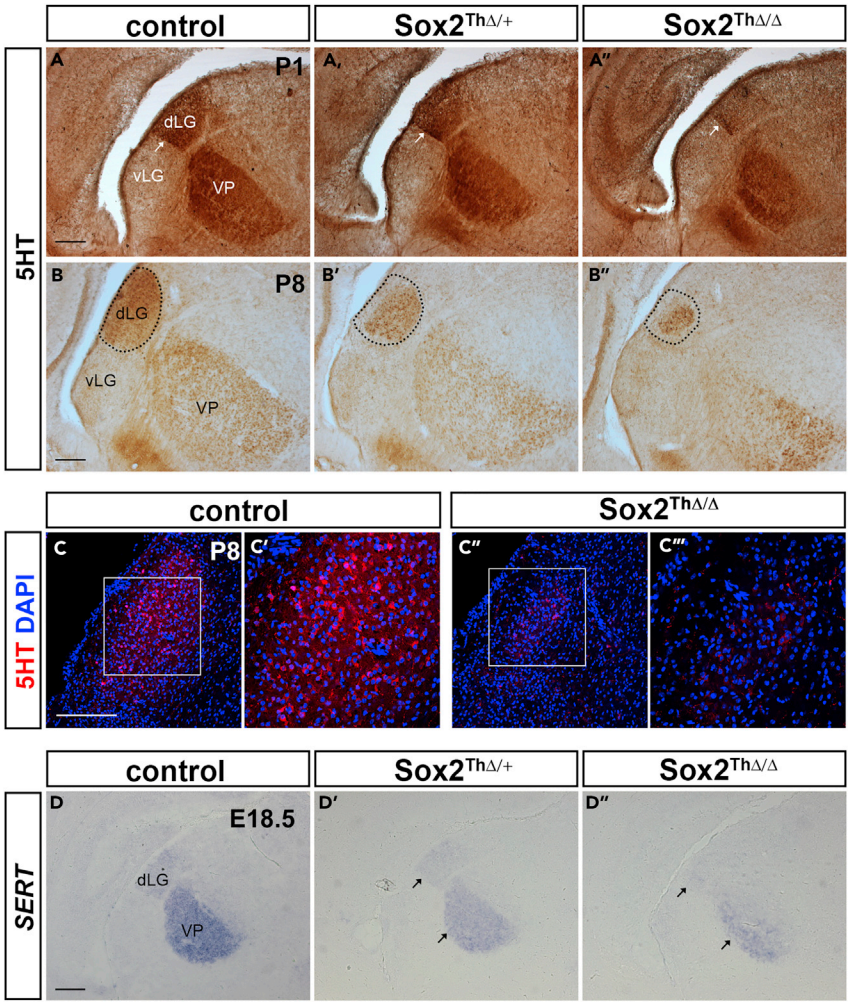

Figure 6. Serotonin Levels in Mutant dLG Are Reduced

(A–B″) Immunohistochemistry for serotonin (5-HT) on coronal sections of Sox2 mutant (A″ and B″), Sox2 heterozygote (A′ and B′), and control (A and B) mouse brains at P1 (A–A″) and P8 (B–B″). The level of serotonin in the dLG is dependent on the number of copies of the Sox2 gene. White arrows indicate the ventral border of the dLG, and dotted lines outline the dLG.

(C–C‴) Immunofluorescence for 5-HT (red) on coronal sections of dLG of Sox2 thalamic mutants (C″ and C‴) and controls (C and C′) at P8. 5-HT levels in the mutant dLG are greatly reduced. Nuclei are marked by DAPI (blue). Note perinuclear 5-HT in controls. C′ and C‴ are magnifications of details in C and C″, respectively (P1 control n = 4, heterozygote n = 3, mutant n = 3; P8 control n = 3, heterozygote n = 2, mutant n = 3).

(D–D″) *In situ* hybridization on coronal sections of E18.5 forebrains of Sox2 homozygote mutant (D″), Sox2 heterozygote (D′), and control (D) with a *SERT* probe. *SERT* is downregulated in the Sox2 mutant thalamus compared with control (black arrows). A mild downregulation is also observed in Sox2 heterozygous thalami indicating a dose-dependent effect of Sox2 loss (control n = 5, heterozygote n = 3, mutant n = 4). Scale bars, 200 μm. dLG, dorso-lateral geniculate nucleus; vLG, ventro-lateral geniculate nucleus; VP, ventro-posterior nucleus.

connectivity also showed abnormal features, suggestive of a more general role for Sox2 in the development of sensory organs-thalamo-cortical connectivity. Within the VP thalamic nucleus, that receives somatosensory input from the periphery and, in turn, projects to the somatosensory cortex, Sox2 is highly expressed in wild-type mice, similarly to the dLGN, but is absent in the Sox2 mutant (Figure 1). We found, by VGlut2 immunohistochemistry, that the map organization of barreloids in the mutant VPN appears perturbed (Figures 7A–7A″). We then visualized TCA from the VP to the somatosensory primary cortex (S1) at P8 by immunohistochemistry for VGlut2 on tangential sections of flattened cortices; we observed that the general topographic organization of the TCA projecting to the S1 area was affected in the mutant cortex. Not

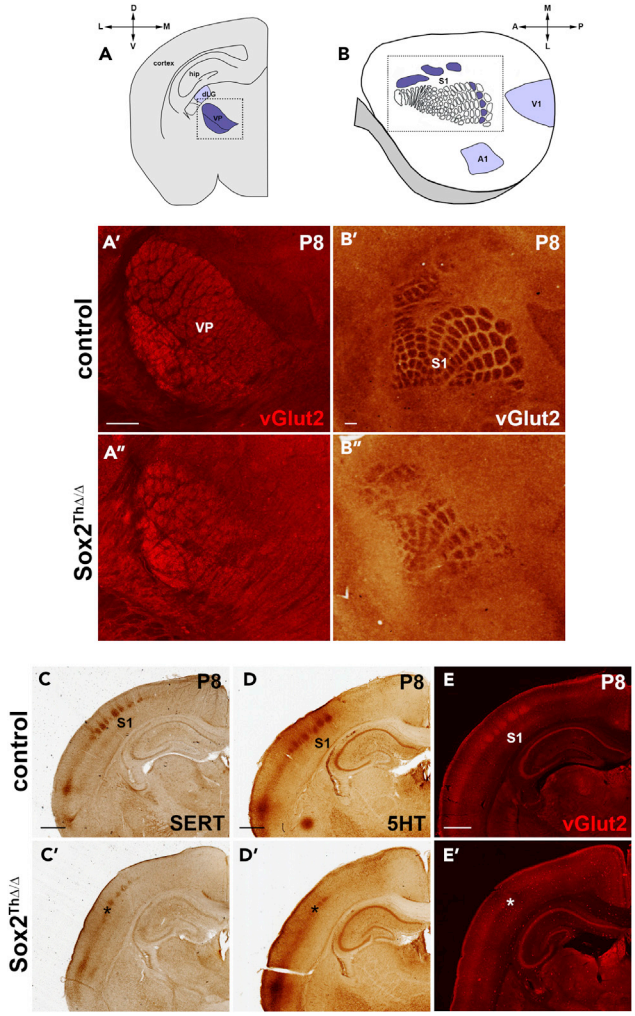

Figure 7. Thalamo-Cortical Somatosensory Afferents and the Somatosensory Thalamic Nucleus (VP) Are Affected

(A–A″) Immunofluorescence for VGlut2 at P8 on coronal section of the VP thalamic nucleus of controls (A′) and Sox2 thalamic mutants (A″). (A) Drawing of a typical coronal section through the thalamus (control n = 4, mutant n = 2).

(B–B″) Immunohistochemistry for VGlut2 of tangential sections of cortical flat mounts (drawing in B) of controls (B′) and Sox2 thalamic mutants (B″) (control n = 16, mutant n = 7).

(C–E′) Immunohistochemistry on coronal sections of mutant and control forebrain at P8 with SERT (C and C′), serotonin (5-HT; D and D′), and VGlut2 (E and E′) antibodies. Barrel fields are not detected in mutant cortex (see *) (SERT control n = 4, mutant n = 2; 5-HT control n = 5, mutant n = 3; VGlut2 control n = 4, mutant n = 2).

Scale bars, 200 μm in (A′–B″) and 600 μm in (C–E′).

VP, ventro-posterior nucleus; S1, primary somatosensory cortex; V1, primary visual cortex; A1, primary auditory cortex; dLG, dorso-lateral geniculate nucleus; hip, hippocampus.

only was VGlut2 staining less intense but also the number of barrel fields, as outlined by VGlut2 staining, was reduced compared with controls (Figures 7B–7B″).

A similar phenotype was observed by immunohistochemistry for SERT, serotonin, and VGlut2 on coronal sections at P8 (Figures 7C–7E′); in particular, cortical barrel fields were less defined and weakly stained (Figures 7C–7E′).

Interestingly, the expression of the Efna5, SERT, and vMAT2 genes, which we had found downregulated in the mutant dLGN, is concomitantly downregulated also in the mutant VP (Figures 5F–5H″, 6, and S3I–S3J″). These findings suggest that at least some of the Sox2-dependent gene regulatory network in the thalamus is shared between different thalamic nuclei.

DISCUSSION

Severe defects of vision are a hallmark of Sox2 deficiency in humans. Known mechanisms underlying the severe visual defects in SOX2 deficiency included, so far, the recognition of the functional importance of SOX2 in the development of retina and crystallin, as revealed by eye-specific mouse conditional KOs (see Introduction). The importance of SOX2 for the development of dLGN and for its retinal or cortical connections demonstrated in this article provide a new, important site of Sox2 function in the visual system, and an additional potential explanation for the visual impairment in SOX2-mutant patients.

The strong expression of SOX2 in postmitotic dLGN projection neurons (Figure 1) was unexpected. In fact, Sox2 functions are critical in stem cells of various types, in particular embryonic, neural, and others, in which it is necessary to preserve stemness (Avilion et al., 2003; Bertolini et al., 2016; Favaro et al., 2009; Kondoh and Lovell-Badge, 2016; Bertolini et al., 2019), and in the reprogramming of differentiated cells to stem cells (Takahashi and Yamanaka, 2016). In contrast, in several neural cell types such as differentiated neurons and glia, Sox2 is either not expressed, or important in very specific cell types, such as retinal Müller glia (Taranova et al., 2006) or cerebellar Bergmann glia (Cerrato et al., 2018).

The development of connectivity between retinal, dLGN, and visual cortex neurons is the result of complex interactions between developing neurons and their environment, involving signaling molecules and their receptors, which are often co-expressed in the growth cones of outgrowing neurons as well as on the target neurons. The possibility to selectively knock out Sox2 in the dLGN (and not the cortex or the retina) with RORα-Cre allowed us to unambiguously attribute the defects observed in mutants in the development of visual connectivity to defects arising, at least primarily, in thalamic neurons, as a result of Sox2 loss.

One important defect consists in a reduction, and a mispatterning, of neuronal afferents from the retina that reach the dLGN (Figures 3 and S2). As Sox2 was not deleted in the developing eye, these defects must primarily depend on defective Sox2 function in the thalamus itself. It is known that retinal innervation plays an important trophic role in dLGN development, particularly in the early postnatal phase (El-Danaf et al., 2015; Guido, 2018), at a time when the Sox2 mutant thalamus fails to continue growing in size as seen in controls (Figure 2 and S2). Thus, the reduced retino-thalamic innervation may contribute to the reduced dLGN size seen postnatally in thalamic Sox2 mutants. KO experiments identified signaling molecules, and their receptors, important for the directional development of axons, and their appropriate targeting. Among these, we find ephrin-A5 to be importantly downregulated in the mutant dLGN (Figure 5). Of note, Efna5 is expressed in both thalamus and retina (Pfeiffenberger et al., 2005), and the KOs that demonstrated the importance of ephrin-A5 for the correct patterning of ipsi- and contralateral eye fibers (Pfeiffenberger et al., 2005) ablated the *Efna5* gene throughout the brain (including thalamus and retina); our results are in agreement with the hypothesis that the *Efna5* gene, regulated by Sox2, plays at least part of its function in retinal axon guidance by acting specifically in the thalamus.

Our finding that SOX2 can directly bind the *Efna5* gene (Figure 5) yields a potential direct Sox2 target within dLGN neurons, and potential regulatory regions for the *Efna5* gene, whose future molecular study could provide insight into dLGN neurons gene regulatory networks.

Sox2-mutant thalamic neurons of the sensory nuclei dLGN (and VP) fail to undergo normal post-natal development, and to generate normal axon outgrowths providing appropriate connections with the cortex (visual and somatosensory, respectively) (Figures 4, 5, and 7). Importantly, these two nuclei are the only ones (with the auditory nucleus) among the many thalamic nuclei that express high levels of Sox2 in neurons. In addition, in Sox2 mutants, both nuclei show decreased expression of genes known to control axon connectivity (ephrin-A5, and SERT) (Figures 5, 6, and S3). In particular, it is known that the knockout of SERT affects VP-originating fibers reaching the somatosensory cortex (Gaspar et al., 2003; Persico et al., 2001; Chen et al., 2015; Teissier et al., 2017); studies of the TCA connecting the dLGN to the visual cortex in SERT mutants were not reported. In Sox2 mutants, the connectivity defects between VP and somatosensory cortex mirror the defect seen in SERT KO mice (Figure 7) (Gaspar et al., 2003; Persico et al., 2001); hence the reduction of SERT and 5-HT expression in Sox2 mutants, together with the altered connections between dLGN with cortical visual areas, and of VP with somatosensory areas, is in agreement with the hypothesis that Sox2-dependent regulation of serotonin transport or metabolism may contribute to sensory TCA connectivity.

It should be noted that additional molecular or cellular defects may be relevant to the abnormal connectivity of thalamic nuclei to the cortex. The observed reduced size of the dLGN (Figure 2), implies a reduction of the number of projections to the cortex (Figure 4). However, the size of the VPN is not, or much less, reduced in mutants, when compared with the dLGN (see Figures 2A–2D′and 6A–6B″), yet thalamic afferents connecting the VPN to the somatosensory cortex (normally forming the barrel fields, see Figure 7, controls) are severely abnormal and disorganized in mutants (Figures 7B–7E′). In addition, the distribution of afferents from the periphery to the VP (forming the barreloids) also appears abnormal (Figures 7A–7A″). Hence, overall, factors other than thalamic nuclear size, specifically conditioning the patterning of neuronal afferents to and from the thalamus, appear to be involved in the observed defects.

Many other defects, such as altered expression of additional signaling molecules, or their receptors, in thalamic neurons, may likely contribute to the alterations observed in Sox2 mutants, and remain to be identified. Future studies of gene expression in mutant thalamic neurons at the genome-wide level (Kalish et al., 2018), will allow to investigate this point in more detail.

A cortical patterning defect in thalamic Sox2 mutants, i.e., the poor definition of V1 and V^{HO} regions of the visual cortex, first pointed to the existence of abnormal TCA in mutants (Figure 4).

Very similar defects were described following thalamic ablation, via RORα-Cre, of *Nr2f1*, a gene whose mutation in humans leads to cerebral visual impairment (Bosch et al., 2014, 2016), raising the question of whether they may functionally interact. We find wide co-expression of SOX2 and NR2F1 in dLGN neurons (not shown); however, we do not detect major alterations in Nr2f1 levels in the mutant dLGN (Figure 5), ruling out that the failure to activate Nr2f1 in dLGN is a key mechanism underlying the defects in Sox2 mutants. The similarities in the phenotype of the two mutants might be due to a general biological process, i.e., a reduction of TCA will always result in V^{HO} patterning defects; due to deregulation of a set of common critical Sox2/Nr2f1 targets, controlling TCA development; or due to a combination of both mechanisms. Future combined studies of Sox2 and Nr2f1 targets will clarify this point.

The identification of Sox2 targets, such as Efna5, SERT, and vMAT2 that are downregulated not only in homozygous Sox2 mutants but also in heterozygotes (Figures 5, 6D, S3, and S4), points to potential candidates for roles in mediating Sox2 function in human visual defects; interestingly, in human patients, heterozygous Sox2 mutation is sufficient to cause blindness, pointing to dosage-sensitive gene regulation by SOX2 as an important phenomenon in the pathogenesis of these defects.

Genetic defects of vision are often polygenic in nature; importantly, some of these defects are dependent on brain, rather than eye, abnormalities (Williamson and FitzPatrick, 2014), but so far SOX2 has only been considered a gene responsible for anophthalmia and microphthalmia, i.e., congenital defects that primarily affect the eye. Our findings raise the possibility that genetically altered Sox2 levels in the thalamus (as obtained by regulatory mutations, or by mutations in Sox2-controlling transcription factors) may also play roles in brain-related visual defects. The importance of Sox2 for gene regulatory networks in the thalamus could allow to identify overlaps with the gene regulatory networks controlled, in the thalamus, by different genes, whose mutation also causes visual disease (as hypothesized for Nr2f1, see above). A better understanding of these networks has the potential to generate new, unifying hypotheses for therapeutic approaches.

Limitations of the Study

Sox2, being a transcription factor, potentially regulates hundreds of genes; it is thus likely that many factors, encoding a variety of molecules affecting the development of neuronal connectivity and dLGN growth in size, are misregulated in Sox2-mutant thalami. The present work identified candidate molecules, based on previous knowledge of their potential effects; it will be necessary to study, by genome-wide RNA sequencing, the alterations of gene expression in mutant versus wild-type dLGN (and VP), to obtain an unbiased catalog of potential effectors of the altered phenotypes. Functional rescue studies will have to be attempted, to confirm the roles in disease of candidate genes.

METHODS

All methods can be found in the accompanying Transparent Methods supplemental file.

SUPPLEMENTAL INFORMATION

Supplemental Information can be found online at https://doi.org/10.1016/j.isci.2019.04.030.

ACKNOWLEDGMENTS

We are grateful to Dr. D. O'Leary for providing the RORα-Cre mouse; Dr. J. Flanagan, Dr. D. Feldheim, Dr. P. Gaspar, Dr. L. Muzio, and Dr. V. Broccoli for ISH probes; and to all members of the Nicolis laboratory and ImprovVision consortium for insightful discussion. Work in the S.K.N. laboratory was funded by the European Community ERANET-NEURON ImprovVision project (also supporting C.F., P.B., and M.S.), Telethon (GGP12152), Associazione Italiana Ricerca sul Cancro (AIRC) (IG-2014), and Cariplo. L.S. was supported by a VINCI PhD fellowship from the Università Italo-Francese/Université Franco-Italienne. P.B. also acknowledges the support of MINECO PCIN-2015-176-C02-01 and BFU2016-75412-R (with FEDER funds). C.F. thanks The Italian Ministry of Health, Mrs. M.C. Regondi for technical support, and Dr. P. Pennacchio for his contribution to early phase of this study.

AUTHOR CONTRIBUTIONS

S.M. and S.K.N. designed the experiments. P.B., C.F., and S.O. contributed to the design, analysis, and discussion of the experiments. S.M., L.S., A.M., and L.G. performed most of the phenotypic analyses. L.S.-A. performed some of the tracing experiments, and P.K. analyzed mutant eye structure and RGC numbers. F.I. and B.F. performed immunohistochemistry experiments and measurements of dLGN size. L.S. and C.B. performed and analyzed transfection experiments. B.M. performed ChIP-seq experiments in F.G.'s laboratory. S.K.N and S.M. prepared the manuscript and figures, with input from all other authors.

DECLARATION OF INTERESTS

The authors declare no competing interests.

Received: February 4, 2019
Revised: April 5, 2019
Accepted: April 23, 2019
Published: May 31, 2019

REFERENCES

Arnold, K., Sarkar, A., Yram, M.A., Polo, J.M., Bronson, R., Sengupta, S., Seandel, M., Geijsen, N., and Hochedlinger, K. (2011). Sox2(+) adult stem and progenitor cells are important for tissue regeneration and survival of mice. Cell Stem Cell *9*, 317–329.

Avilion, A.A., Nicolis, S.K., Pevny, L.H., Perez, L., Vivian, N., and Lovell-Badge, R. (2003). Multipotent cell lineages in early mouse development depend on SOX2 function. Genes Dev. *17*, 126–140.

Bertolini, J., Mercurio, S., Favaro, R., Mariani, J., Ottolenghi, S., and Nicolis, S.K. (2016). Sox2-dependent regulation of neural stem cells and CNS development. In Sox2, Biology and Role in Development and Disease, H. Kondoh and R. Lovell-Badge, eds. (Elsevier), pp. 187–216.

Bertolini, J.A., Favaro, R., Zhu, Y., Pagin, M., Ngan, C.Y., Wong, C.H., Tjong, H., Vermunt, M.W., Martynoga, B., Barone, C., et al. (2019). Mapping the global chromatin connectivity network for Sox2 function in neural stem cell maintenance. Cell Stem Cell *24*, 462–476.e6.

Bosch, D.G., Boonstra, F.N., de Leeuw, N., Pfundt, R., Nillesen, W.M., de Ligt, J., Gilissen, C., Jhangiani, S., Lupski, J.R., Cremers, F.P., and De Vries, B.B. (2016). Novel genetic causes for cerebral visual impairment. Eur. J. Hum. Genet. *24*, 660–665.

Bosch, D.G., Boonstra, F.N., Gonzaga-Jauregui, C., Xu, M., de Ligt, J., Jhangiani, S., Wiszniewski, W., Muzny, D.M., Yntema, H.G., Pfundt, R., et al. (2014). NR2F1 mutations cause optic atrophy with intellectual disability. Am. J. Hum. Genet. *94*, 303–309.

Braisted, J.E., Catalano, S.M., Stimac, R., Kennedy, T.E., Tessier-Lavigne, M., Shatz, C.J., and O'Leary, D.D. (2000). Netrin-1 promotes thalamic axon growth and is required for proper development of the thalamocortical projection. J. Neurosci. *20*, 5792–5801.

Cerrato, V., Mercurio, S., Leto, K., Fuca, E., Hoxha, E., Bottes, S., Pagin, M., Milanese, M., Ngan, C.Y., Concina, G., et al. (2018). Sox2 conditional mutation in mouse causes ataxic symptoms, cerebellar vermis hypoplasia, and postnatal defects of Bergmann glia. Glia *66*, 1929–1946.

Chen, X., Ye, R., Gargus, J.J., Blakely, R.D., Dobrenis, K., and Sze, J.Y. (2015). Disruption of transient serotonin accumulation by non-serotonin-producing neurons impairs cortical map development. Cell Rep. *10*, 346–358.

Chou, S.J., Babot, Z., Leingartner, A., Studer, M., Nakagawa, Y., and O'Leary, D.D. (2013). Geniculocortical input drives genetic distinctions between primary and higher-order visual areas. Science *340*, 1239–1242.

El-Danaf, R.N., Krahe, T.E., Dilger, E.K., Bickford, M.E., Fox, M.A., and Guido, W. (2015). Developmental remodeling of relay cells in the dorsal lateral geniculate nucleus in the absence of retinal input. Neural Dev. *10*, 19.

Fantes, J., Ragge, N.K., Lynch, S.A., Mcgill, N.I., Collin, J.R., Howard-Peebles, P.N., Hayward, C., Vivian, A.J., Williamson, K., Van Heyningen, V., and Fitzpatrick, D.R. (2003). Mutations in SOX2 cause anophthalmia. Nat. Genet. *33*, 461–463.

Favaro, R., Valotta, M., Ferri, A.L., Latorre, E., Mariani, J., Giachino, C., Lancini, C., Tosetti, V., Ottolenghi, S., Taylor, V., and Nicolis, S.K. (2009). Hippocampal development and neural stem cell maintenance require Sox2-dependent regulation of Shh. Nat. Neurosci. *12*, 1248–1256.

Ferri, A., Favaro, R., Beccari, L., Bertolini, J., Mercurio, S., Nieto-Lopez, F., Verzeroli, C., La Regina, F., de Pietri Tonelli, D., Ottolenghi, S., et al. (2013). Sox2 is required for embryonic development of the ventral telencephalon through the activation of the ventral determinants Nkx2.1 and Shh. Development *140*, 1250–1261.

Garel, S., and Lopez-Bendito, G. (2014). Inputs from the thalamocortical system on axon pathfinding mechanisms. Curr. Opin. Neurobiol. *27*, 143–150.

Gaspar, P., Cases, O., and Maroteaux, L. (2003). The developmental role of serotonin: news from mouse molecular genetics. Nat. Rev. Neurosci. *4*, 1002–1012.

Gezelius, H., and Lopez-Bendito, G. (2017). Thalamic neuronal specification and early circuit formation. Dev. Neurobiol. *77*, 830–843.

Graham, V., Khudyakov, J., Ellis, P., and Pevny, L. (2003). SOX2 functions to maintain neural progenitor identity. Neuron *39*, 749–765.

Guido, W. (2018). Development, form, and function of the mouse visual thalamus. J. Neurophysiol. *120*, 211–225.

Horng, S., Kreiman, G., Ellsworth, C., Page, D., Blank, M., Millen, K., and Sur, M. (2009). Differential gene expression in the developing lateral geniculate nucleus and medial geniculate nucleus reveals novel roles for Zic4 and Foxp2 in visual and auditory pathway development. J. Neurosci. *29*, 13672–13683.

Huberman, A.D., Murray, K.D., Warland, D.K., Feldheim, D.A., and Chapman, B. (2005). Ephrin-As mediate targeting of eye-specific projections to the lateral geniculate nucleus. Nat. Neurosci. *8*, 1013–1021.

Kalish, B.T., Cheadle, L., Hrvatin, S., Nagy, M.A., Rivera, S., Crow, M., Gillis, J., Kirchner, R., and Greenberg, M.E. (2018). Single-cell transcriptomics of the developing lateral geniculate nucleus reveals insights into circuit assembly and refinement. Proc. Natl. Acad. Sci. U S A *115*, E1051–E1060.

Kamachi, Y., Uchikawa, M., Tanouchi, A., Sekido, R., and Kondoh, H. (2001). Pax6 and SOX2 form a co-DNA-binding partner complex that regulates initiation of lens development. Genes Dev. *15*, 1272–1286.

Kania, A., and Klein, R. (2016). Mechanisms of ephrin-Eph signalling in development, physiology and disease. Nat. Rev. Mol. Cell Biol. *17*, 240–256.

H. Kondoh, and R. Lovell-Badge, eds. (2016). Sox2, Biology and Role in Development and Disease (Elsevier, Associated Press).

Lebrand, C., Cases, O., Adelbrecht, C., Doye, A., Alvarez, C., El Mestikawy, S., Seif, I., and Gaspar, P. (1996). Transient uptake and storage of serotonin in developing thalamic neurons. Neuron *17*, 823–835.

Lee, K.E., Seo, J., Shin, J., Ji, E.H., Roh, J., Kim, J.Y., Sun, W., Muhr, J., Lee, S., and Kim, J. (2014). Positive feedback loop between Sox2 and Sox6 inhibits neuronal differentiation in the developing central nervous system. Proc. Natl. Acad. Sci. U S A *111*, 2794–2799.

Little, G.E., Lopez-Bendito, G., Runker, A.E., Garcia, N., Pinon, M.C., Chedotal, A., Molnar, Z., and Mitchell, K.J. (2009). Specificity and plasticity of thalamocortical connections in Sema6A mutant mice. PLoS Biol. *7*, e98.

Mariani, J., Favaro, R., Lancini, C., Vaccari, G., Ferri, A.L., Bertolini, J., Tonoli, D., Latorre, E., Caccia, R., Ronchi, A., et al. (2012). Emx2 is a dose-dependent negative regulator of Sox2 telencephalic enhancers. Nucleic Acids Res. *40*, 6461–6476.

Miyashita-Lin, E.M., Hevner, R., Wassarman, K.M., Martinez, S., and Rubenstein, J.L. (1999). Early neocortical regionalization in the absence of thalamic innervation. Science *285*, 906–909.

Panaliappan, T.K., Wittmann, W., Jidigam, V.K., Mercurio, S., Bertolini, J.A., Sghari, S., Bose, R., Patthey, C., Nicolis, S.K., and Gunhaga, L. (2018). Sox2 is required for olfactory pit formation and olfactory neurogenesis through BMP restriction and Hes5 upregulation. Development *145*, https://doi.org/10.1242/dev.153791.

Persico, A.M., Mengual, E., Moessner, R., Hall, F.S., Revay, R.S., Sora, I., Arellano, J., Defelipe, J., Gimenez-Amaya, J.M., Conciatori, M., et al. (2001). Barrel pattern formation requires serotonin uptake by thalamocortical afferents, and not vesicular monoamine release. J. Neurosci. *21*, 6862–6873.

Pevny, L.H., and Nicolis, S.K. (2010). Sox2 roles in neural stem cells. Int. J. Biochem. Cell Biol. *42*, 421–424.

Pfeiffenberger, C., Cutforth, T., Woods, G., Yamada, J., Renteria, R.C., Copenhagen, D.R., Flanagan, J.G., and Feldheim, D.A. (2005). Ephrin-As and neural activity are required for eye-specific patterning during retinogeniculate mapping. Nat. Neurosci. *8*, 1022–1027.

Seabrook, T.A., Burbridge, T.J., Crair, M.C., and Huberman, A.D. (2017). Architecture, function, and assembly of the mouse visual system. Annu. Rev. Neurosci. *40*, 499–538.

Smith, A.N., Miller, L.A., Radice, G., Ashery-Padan, R., and Lang, R.A. (2009). Stage-dependent modes of Pax6-Sox2 epistasis regulate lens development and eye morphogenesis. Development *136*, 2977–2985.

Sur, M., and Rubenstein, J.L. (2005). Patterning and plasticity of the cerebral cortex. Science *310*, 805–810.

Takahashi, K., and Yamanaka, S. (2016). A decade of transcription factor-mediated reprogramming to pluripotency. Nat. Rev. Mol. Cell Biol. *17*, 183–193.

Taranova, O.V., Magness, S.T., Fagan, B.M., Wu, Y., Surzenko, N., Hutton, S.R., and Pevny, L.H. (2006). SOX2 is a dose-dependent regulator of retinal neural progenitor competence. Genes Dev. *20*, 1187–1202.

Teissier, A., Soiza-Reilly, M., and Gaspar, P. (2017). Refining the role of 5-HT in postnatal development of brain circuits. Front. Cell. Neurosci. *11*, 139.

Vanderhaeghen, P., Lu, Q., Prakash, N., Frisen, J., Walsh, C.A., Frostig, R.D., and Flanagan, J.G. (2000). A mapping label required for normal scale of body representation in the cortex. Nat. Neurosci. *3*, 358–365.

Williamson, K.A., and FitzPatrick, D.R. (2014). The genetic architecture of microphthalmia, anophthalmia and coloboma. Eur. J. Med. Genet. *57*, 369–380.

ISCI, Volume *15*

Supplemental Information

Sox2 Acts in Thalamic Neurons to Control the Development of Retina-Thalamus-Cortex Connectivity

Sara Mercurio, Linda Serra, Alessia Motta, Lorenzo Gesuita, Luisa Sanchez-Arrones, Francesca Inverardi, Benedetta Foglio, Cristiana Barone, Polynikis Kaimakis, Ben Martynoga, Sergio Ottolenghi, Michèle Studer, Francois Guillemot, Carolina Frassoni, Paola Bovolenta, and Silvia K. Nicolis

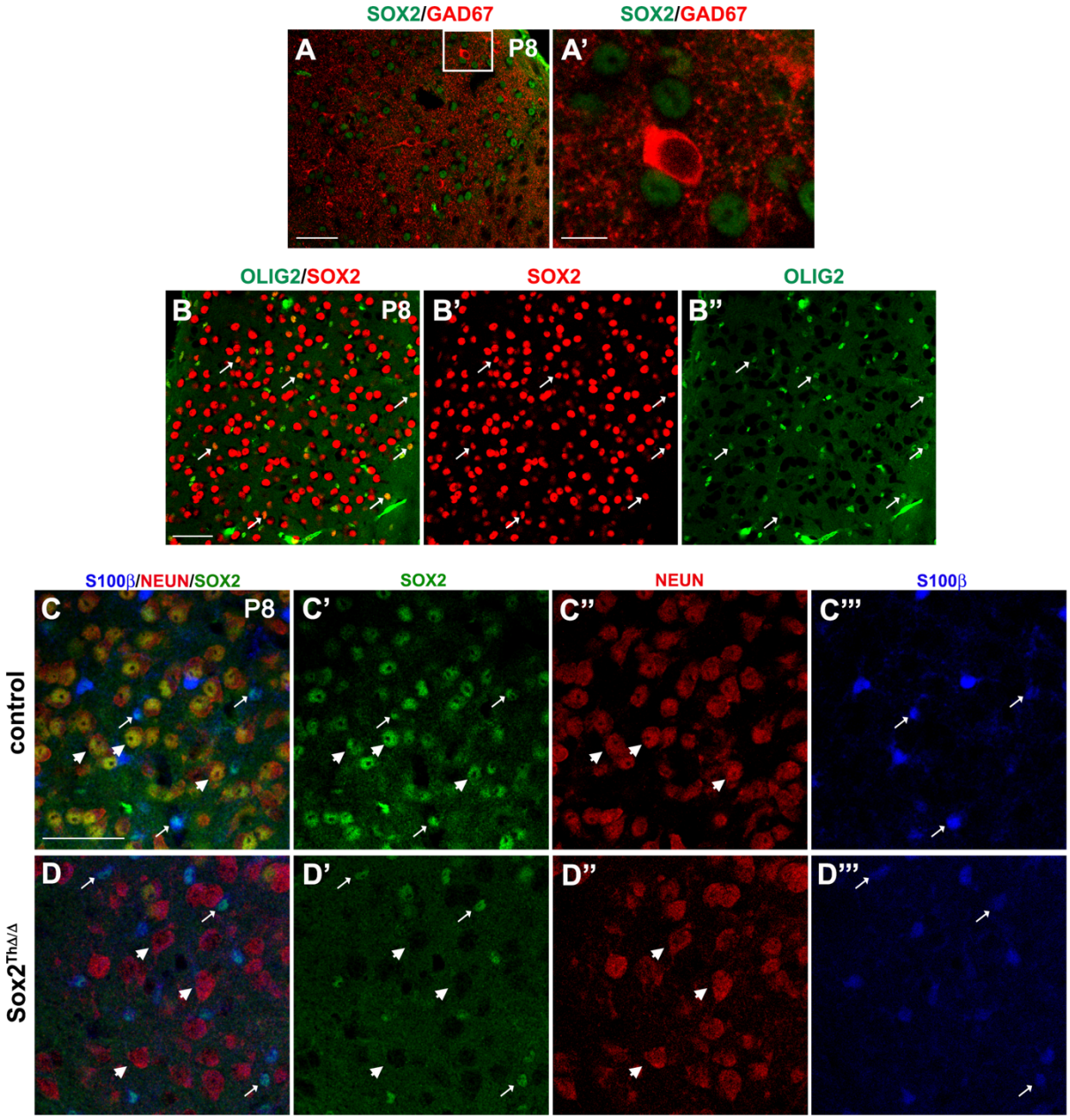

Figure S1. Related to Figure 1. SOX2 is not expressed in GABAergic interneurons and in the large majority of oligodendrocytes in dLG. (A-A') Immunofluorescence on coronal sections of dLG of mouse brain at P8 with anti-SOX2 (green) and anti-GAD67 (red) (a GABAergic interneuron marker), antibodies. SOX2 is not expressed in GABAergic interneurons in dLG (n=3). **(B-B'')** Immunofluorescence on coronal sections of dLG of mouse brain at P8 with anti-SOX2 (red) and anti-OLIG2 (green) (an oligodendroglial marker), antibodies. SOX2 is expressed in a few oligodendrocytes (arrows). (n=3). **(C-D''')** Immunofluorescence on coronal sections of dLG at P8 of controls and Sox2 thalamic mutants with anti-SOX2 (green; C',D'), anti-NEUN (red; C'',D'') and anti-S100β (blue; C''',D'''). SOX2 expression in the mutant dLG is ablated in neurons (arrow heads) but remains in some S100β-positive cells (arrows) (control n=3, mutant n=3).
Scale bars: 50µm (A,B-D'''), 10µm (A'). dLG, dorso lateral geniculate nucleus.

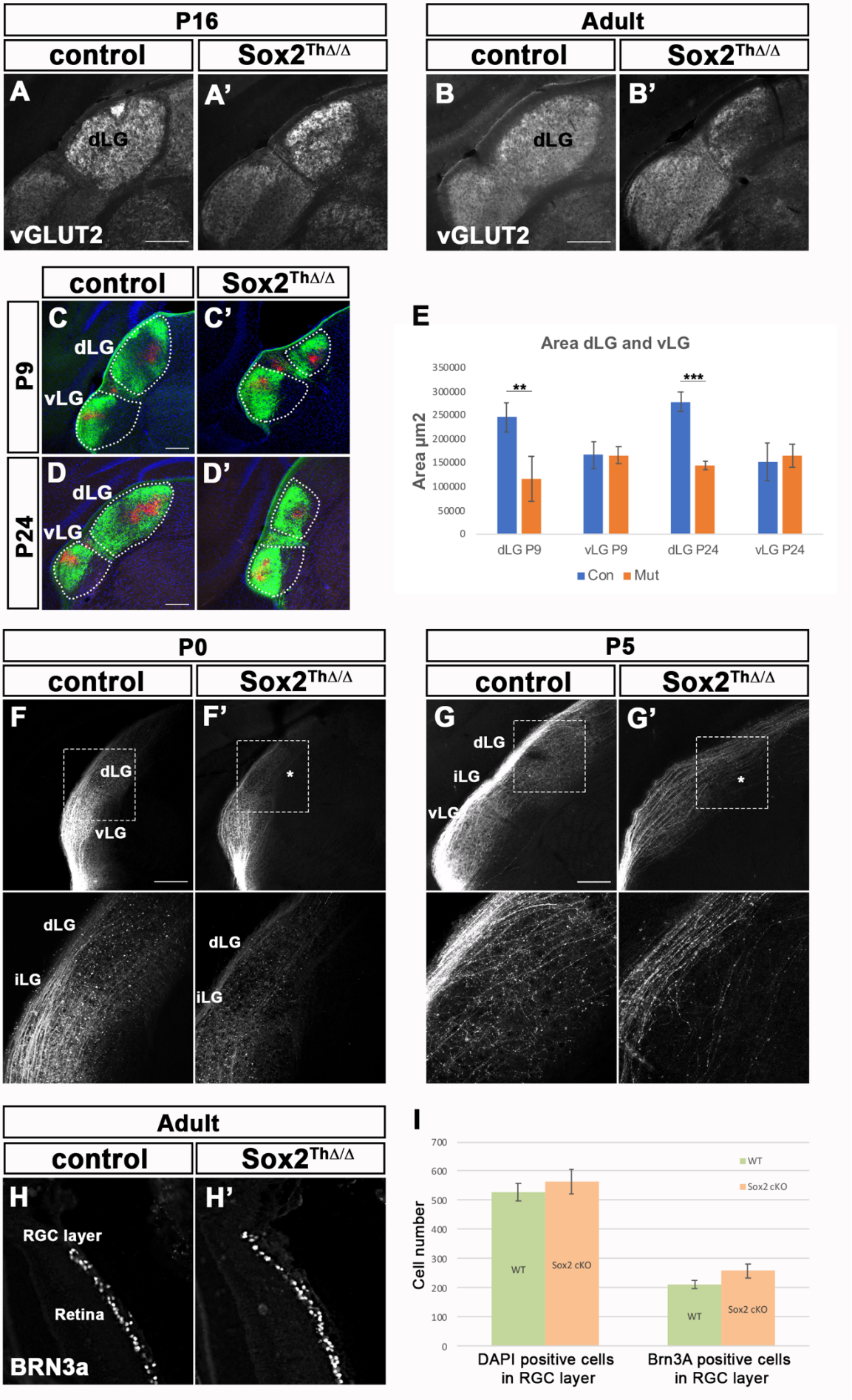
P16
control
Sox2ThΔ/Δ
A
A'
dLG
vGLUT2
Adult
control
Sox2ThΔ/Δ
B
B'
dLG
vGLUT2
control
Sox2ThΔ/Δ
P9
P24
C
C'
D
D'
dLG
vLG
E
Area dLG and vLG
Area µm2
350000
300000
250000
200000
150000
100000
50000
0
**
***
dLG P9
vLG P9
dLG P24
vLG P24
Con
Mut
P0
control
Sox2ThΔ/Δ
F
F'
dLG
vLG
iLG
*
P5
control
Sox2ThΔ/Δ
G
G'
dLG
iLG
vLG
*
Adult
control
Sox2ThΔ/Δ
H
H'
RGC layer
Retina
BRN3a
I
Cell number
700
600
500
400
300
200
100
0
WT
Sox2 cKO
DAPI positive cells in RGC layer
Brn3A positive cells in RGC layer

Figure S2. Related to Figure 2 and Figure 3.
Sox2 thalamic ablation affects the development of the dLG and retino-geniculate projections but not the final number of adult RGC. (A-B') Anti-vGLUT2 immunofluorescence on coronal sections of control and mutant dLG at P16 (control n=2, mutant n=2) (A,A') and in adult (control n=2, mutant n=2) (B,B') shows a reduction of retinal afferents and of the dLG size in Sox2 mutants. (**C-E**) Representative coronal vibratome sections used to measure dLG and vLG size at P9 and P24 in which retinal afferents had been marked with CTB. Dotted lines outline the dLG and vLG nuclei total area. (E) Histogram comparing the quantification of dLG and vLG areas in mutants and controls. The dLG size was reduced in Sox2 thalamic mutants at P9 (** $p<0.01$, unpaired Student's T-test, control n=3, mutant n=4) and P24 (*** $p<0.005$, unpaired Student's T-test, control n=3, mutant n=3), while vLG appears unchanged. Error bars represent standard deviation.
(F-G') Tracing experiment by inserting DiI crystal in the eye at P0 (control n=3, mutant n=3) (F,F') and P5 (control n=2, mutant n=2) (G,G') shows a reduction and defasiculation of retinal axons (indicated by *) reaching the dLG in mutants (F',G') compared to controls (F,G).
(H-I) Anti-BRN3A immunofluorescence on coronal sections of adult mutant and control retina marking retinal ganglion cells (RGC). (I) Quantification of RGC does not show any difference in number between controls and Sox2 mutants (n=3). Error bars represent standard deviation. Scale bars: 250µm (A-B', F-G'), 200 µm (C-D').
dLG, dorso lateral geniculate nucleus; vLG, ventro lateral geniculate nucleus; iLG, intermediate lateral geniculate nucleus; RGC, retinal ganglion cell.

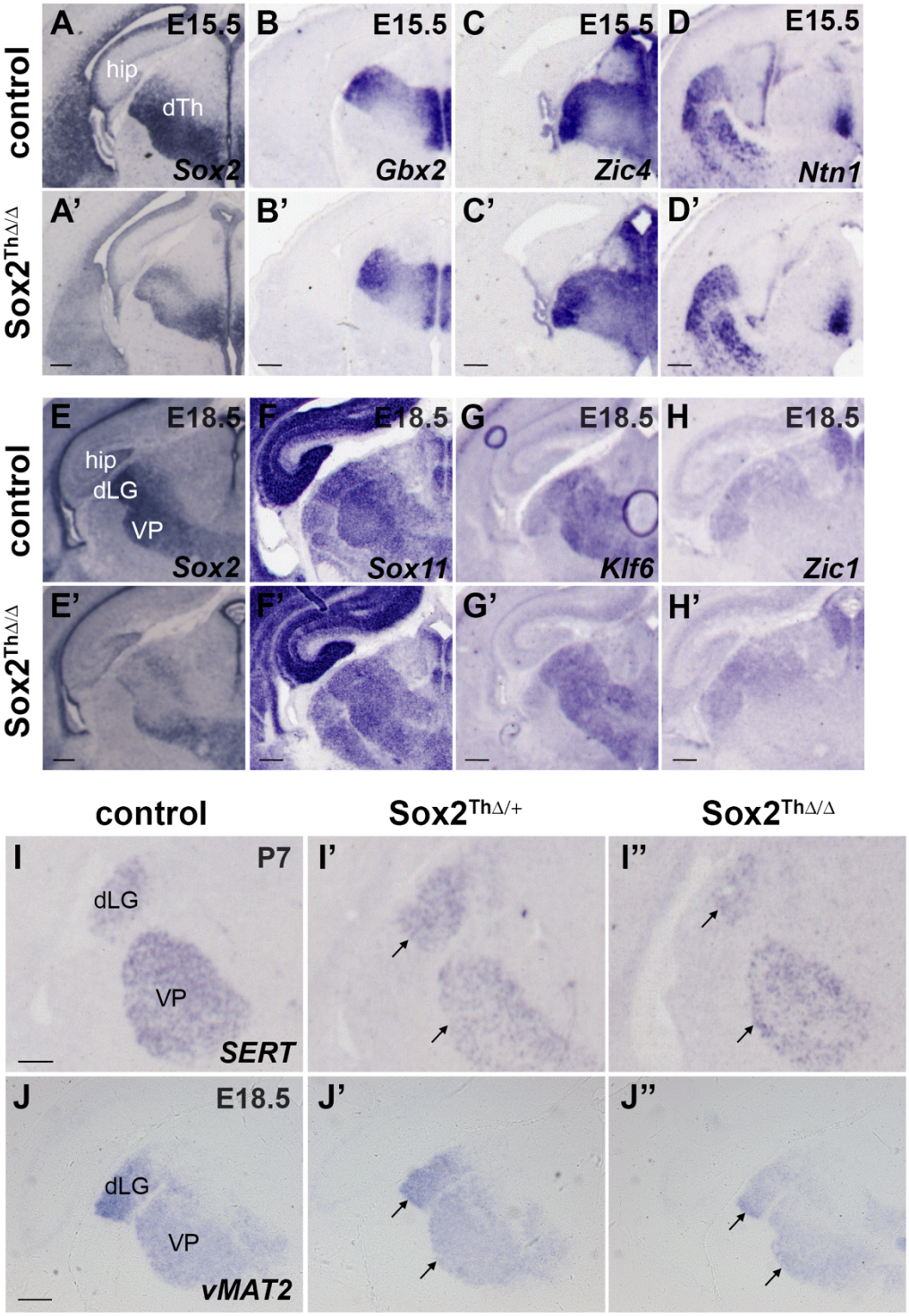

Figure S3. Related to Figure 5 and Figure 6.
Expression of key regulators of the development of the visual system. (A-D') *In situ* hybridization on coronal sections of mutant and control mouse forebrains at E15.5 with *Sox2*, *Gbx2*, *Zic4* and *Netrin1* probes. (At least 3 controls and 2 mutants were analysed for each probe). **(E-H')** *In situ* hybridization on coronal sections of mutant and control mouse forebrains at E18.5 for *Sox2*, *Sox11*, *Klf6* and *Zic1* expression (At least 3 controls and 2 mutants were analysed for each probe). **(I-J")** *In situ* hybridization on coronal sections of forebrains of Sox2 homozygote mutants, Sox2 heterozygotes and controls at P7 and E18.5 with the serotonin transporters *SERT* (control n=2, mutant n=3) (I-I") and *vMAT2* (control n=9, mutant n=5) (J-J"). Arrows indicate *SERT* and *vMAT* downregulation in dLG (and VP). Scale bars 200µm.
hip, hippocampus; dLG, dorso-lateral geniculate nucleus; VP, ventroposterior nucleus; dTh, dorsal thalamus.

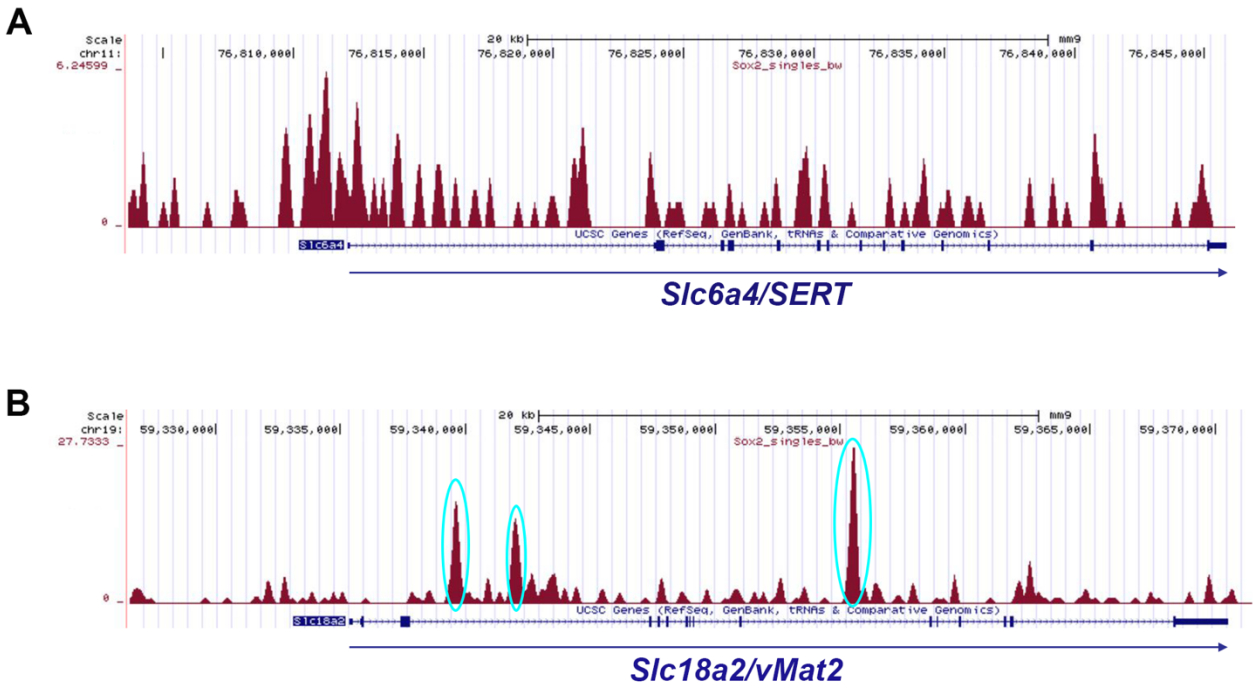

Figure S4. Related to Figure 6.
SOX2 ChIPseq detects SOX2 binding to the SERT- and vMAT2-encoding genes.
SOX2 ChIPseq profile from neurosphere cultures derived from postnatal mouse telencephalon across the *Slc6a4/SERT* locus **(A)** and the *Slc18a2/vMAT2* locus **(B)** showing 3 SOX2 peaks in the *Slc18a2/vMAT2* locus (blue circles). N.B. SOX2 binding to the *Slc6a4/SERT* locus was not detected by the peak calling algorithm. Note the different scale of the Y axis in A and B.

Transparent Methods

Mouse strains

Mutant mice (sex was indifferent) were obtained by crossing the following mouse lines: $Sox2^{Flox}$ (Favaro et al., 2009) with Rorα-Cre (Chou et al., 2013). The day of vaginal plug was defined as embryonic day 0 (E0) and the day of birth as postnatal day 0 (P0). Genotyping was performed with the following primers: Rorα-Cre IRES Forward: 5'AGGAATGCAAGGTCTGTTGAAT 3'; Rorα-Cre IRES Reverse: 5' TTTTTCAAAGGAAAACCACGTC 3'; Sox2 Flox Forward: 5'AAGGTACTGGGAAGGGACATTT 3'; Sox2 Flox Reverse: 5'AGGCTGAGTCGGGTCAATTA 3'

All procedures were in accordance with the European Communities Council Directive (2010/63/EU and 86/609/EEC) regulating animal research, and the Italian Law for Care and Use of Experimental Animals (DL26/14). They were approved by the Italian Ministry of Health (authorization no. 189/2016-PR to Prot. 29C09.4) and the Bioethics Subcommittee of Consejo Superior de Investigaciones Científicas (CSIC, Madrid, Spain) and the Comunidad de Madrid (protocol approval number PROEX 100/15; RD 53/2013).

In situ hybridization

In situ hybridization on sections was performed essentially as in (Cerrato et al., 2018). Briefly, embryonic brains and P0 brains were dissected and fixed overnight in paraformaldehyde 4% in PBS (Posphate Buffered Saline) (PFA 4%). For P1 brains and older, animals were first perfused with PFA 4% and brains were then extracted and fixed as above. The fixed tissue was cryoprotected in a series of sucrose solutions in PBS (15%, 30%) and then embedded in OCT (Killik, Bio-Optica) and stored at -80°C. Brains were sectioned (20 µm) with a cryostat, placed on a slide (Super Frost Plus 09-OPLUS, Menzel) and stored at -80°C. Slides were then defrosted, fixed in formaldehyde 4% in PBS for 10 minutes (min), washed 3 times for 5 min in PBS, incubated for 10 min in acetylation solution (for 200 ml: 2.66 ml triethanolamine, 0.32 ml HCl 37%, 0.5 ml acetic anhydride 98%) with constant stirring and then washed 3 times for 5 min in PBS. Slides were placed in a humid chamber and covered with prehybridization solution (50% formamide, 5X SSC, 0.25 mg/ml tRNA, 5X Denhardt's, 0.5 µg/ml salmon sperm) for at least 2 hours (h) and then incubated in hybridization solution (fresh prehybridization solution containing the digoxygenin (DIG)-labelled RNA probe of interest) overnight at 65°C. Slides were washed 5 min in 5X SSC, incubated 2 times in 0.2X SSC for 30 min at 65°C, washed 5 min in 0.2X SSC at room temperature and then 5 min in Maleic Acid Buffer (MAB, 100 mM maleic acid, 150 mM NaCl pH 7.5). The slides were incubated in blocking solution (10% sheep serum, 2% blocking reagent (Roche), 0.3% Tween-20 in MAB) for at least 1 h

at room temperature, then covered with fresh blocking solution containing anti-DIG antibody Roche © 1:2000 and finally placed overnight at 4°C. Slides were washed in MAB 3 times for 5 min, in NTMT solution (100 mM NaCl, 100 mM Tris-HCl pH 9.5, 50 mM $MgCl_2$, 0.1% Tween-20) 2 times for 10 min and then placed in a humid chamber, covered with BM Purple (Roche), incubated at 37°C until desired staining was obtained (1-6 h), washed in water for 5 min, air dried and mounted with Eukitt (Sigma).

For *in situ* hybridization on whole mounts (WM), brains were dissected and fixed, after removing the meninges, in PFA 4% overnight at 4°C. Brains were dehydrated in a methanol series (25%, 50% in PBS, followed by 75% in water, 100%), and stored at -20°C until used. Brains were rehydrated at room temperature, and incubated in 6% H_2O_2 in PTW (1% Tween-20 in PBS) for 1 h at room temperature; they were washed two times for 15 min in PTW and then incubated with proteinase K (20 µg/ml) for 1 h. Brains were further washed two times quickly in PTW, post-fixed in 0.2% glutaraldehyde, 4% formaldehyde in PTW for 20 min at room temperature. Prehybridization (prehyb, 1 ml/brain) WM was then performed by incubating in prehyb WM solution (50% formamide, 5X SSC pH 4.5, 20% SDS, 500 µg/ml tRNA, 200 µg/ml BSA, 50 µg/ml heparin) for 2-3 h at 70°C (individually in closed glass or plastic vials in an oven). Solution was changed to 1 ml/brain hybridization WM solution (prehyb WM solution with added DIG-labelled RNA probe, final dilution of 1:50-1:100 starting from a 120 µl probe solution [20 µl standard probe synthesis reaction + 100 µl prehyb solution]) and incubated for 16-20 h at 70°C. Brains were then washed in solution X (2X SSC pH 4.5, 50% formamide, 1% SDS) at 70°C 4 times for 45 min each, then in MABT (Maleic Acid Buffer –see above- + 1% Tween 20), 3 times (10 min each) at room temperature. The buffer was then changed to blocking solution (10% sheep serum, 2% Roche © blocking reagent in MABT), and incubated for 2 h at room temperature. This was then replaced with anti-DIG solution (anti-DIG antibody Roche © 1:4000 in blocking solution) and incubated overnight at 4°C. Brains were transferred to 12-well plates (1 brain/well) and washed in MABT (3 washes of 10 min each, then 5 washes of 1h each, and one overnight wash at 4°C), followed by incubation in NTMT WM buffer (100 mM NaCl, 100 mM Tris-HCl pH 9.5, 50 mM $MgCl_2$, 1% Tween 20) at room temperature for two washes of 10 minutes each, and incubation at room temperature in the dark in NBT-BCIP colour reaction solution (3.5 µl NBT, 3.5 µl BCIP, per each ml of NTMT WM; about 3 ml per well), until signal appearance (usually about 2-6 h). The reaction was then blocked with TE stop buffer (10 mM TrisHcl pH 7.5, 10 mM EDTA pH 8), by 2 washes of at least 2 h at room temperature. To improve the signal/background ratio, brains were then cleared in glass vials with a sequence of the following solutions: PBS 2 times quickly, 50%

methanol in PBS for 1 h, 100% methanol for 1 h 3 times, 1:1 volume methanol:clearing solution (1:2 volume benzyl alcohol, benzyl benzoate) for 1 h at room temperature, and finally in clearing solution overnight to one week, when tissue should show a clear and clean signal; then, the same washes were performed in reverse, until PBS. Brains were then photographed under a stereomicroscope.

The following DIG-labelled probes were used: *Sox2* (Favaro et al., 2009), *Lef1* (Muzio et al., 2005), *Efna5* (Huberman et al., 2005, Pfeiffenberger et al., 2005) (a gift from J. Flanagan and D. Feldheim, giving equivalent results), *Bhlhb5* (Alfano et al., 2014), *Lmo4* (Chou et al., 2013), *Nr2f1* (Armentano et al., 2007), *Sox11* (a gift from P. Sharpe), *SERT/Slc6a4* (Lebrand et al 1996) (a gift from P. Gaspar), *Semaphorin6A* (Kerjan et al., 2005), *Gbx2* (Li et al., 2002), *Netrin1* (Livnat et al., 2010) and we cloned from brain cDNAs (E14.4 or P30 telencephalon) of *Zic1* (using primers from (Gaston-Massuet et al., 2005), *Zic4* (using primers from (Horng et al., 2009)), *NetrinG1*, *Klf6* and *vMAT2/Slc18a2* (using the primers provided from http://portal.brain-map.org/).

Immunohistochemistry and cell counting

Immunohistochemistry with anti-vGLUT2 (rabbit polyclonal, Synaptic systems cat. no.135402, lot no. 135402/25, 1:1000), anti-serotonin (5HT) (rabbit polyclonal, Immunostar cat. no. 20080, 1:2000), and anti-SERT (rabbit polyclonal, Immunostar cat. no. 24330, 1:2000) antibodies on P1 and P8 brains was carried out on coronal cryostat sections (40 µm for P1 and 50 µm for P8) collected in 24-well plates filled with PBS. Immunohistochemistry with anti-vGLUT2 and anti-SERT antibodies was also carried out on tangential cryostat sections of P8 flattened cortices (50 µm) also collected in 24-well plates filled with PBS. Sections were washed in H_2O_2 3% in PBS for 15 min after quick washes in PBS they were incubated in PBS+ (PBS, gelatin 0.2%, Triton X-100 0.25%) for at least 1 h. PBS+ was replaced with PBS+ containing the antibody of interest and sections were incubated overnight at room temperature. Sections were washes 4 times in PBS+, 15 minutes each, and then incubated in PBS+ containing the biotinylated secondary antibody 1:200 (ABC Vector Kit Vectastain) 2 h at room temperature. Sections were washed 4 times, 15 min each, in PBS+, incubated with ABC working solution (ABC Vector Kit Vectastain) 1 h and 30 min at room temperature and then washed in PBS containing Triton X-100 0.25% 3 times, 15 min each and then left washing overnight at 4°C. They were washed in PBS, Triton X-100 0.25% for 15 min, then washed twice in PBS and finally incubated in Tris-HCl 0.05M pH 7.5 for 10 minutes. Sections were placed in DAB (3,3'-diamiobenzidine tetrahydrochloride, Sigma) staining solution (DAB 0.075%, H_2O_2 0.002% in Tris-HCl 0.05M pH 7.5). When desired staining was obtained (usually

after 10-30 min) the reaction was blocked with PBS washes. Sections were placed on slides (Super Frost Plus 09-OPLUS, Menzel), dried and mounted with Eukitt (Sigma). Immunofluorescence with anti-vGLUT2 and anti-5HT on P8 and P16 coronal cryostat sections was carried out essentially as above with the following alterations: the H_2O_2 treatment was skipped, sections were incubated with anti-rabbit Alexa 546 secondary antibody (Invitrogen 1:800) and after the PBS washes sections were directly mounted on slides with Fluormount (Sigma) containing DAPI. Retinal ganglion cell (RGC) counting was performed on cryostat sections (20μm) from enucleated eyes. Animals were perfused as described above and then eyes were enucleated maintaining a piece of the eye lid for orientation, post-fixed overnight at 4°C and cryoprotected in sucrose solutions and embedded in OCT, as described above. Sections were subjected to immunohistochemistry as described above using the RGC marker BRN3a (Santa Cruz; cat. no. SC-31984, lot no. D2915, 1:1000).
Selected free-floating P8 coronal vibratome sections (50μm thick) were blocked in PBS containing 1% bovine adult serum (BSA, Sigma) and 0.2% Triton-X 100 for 2 h and, subsequently, incubated overnight at 4°C with mouse or goat anti-Sox2 (R&D MAB 2018, 1:50 or R&D AF2018, 1:200) combined with one of the following antibodies: guinea pig anti-NEUN (Chemicon, Temecula, CA, USA,1:2000), rabbit anti-S100β (Dako, Glostrup, Denmark. 1:1000), goat anti-GAD67 (R&D, 1:200), mouse anti-OLIG2 (Merk Millipore, Billerica,Mass,USA;1:500). After PBS washes, sections were incubated for 2 h in a mixture of the corresponding indo-carbocyanine Cy3 or Cy2-conjugated secondary antibodies (Jackson ImmunoResearch Laboratories, West Grove, Pa., USA; 1:600). Sections were then counterstained with 4,6-diamidino-2-phenylindole (DAPI; Molecular Probes, Eugene, OR, USA; 1:1000), mounted with Fluorsave (Calbiochem, San Diego, CA, USA), and imaged with a confocal microscope D-Eclipse C1 (Nikon, Tokyo, Japan). Confocal images were acquired using small pinhole aperture size and low gain and offset to prevent saturation and imported into Adobe Photoshop CS5 (Adobe Systems Incorporated, San Jose, CA, USA) after adjustment of contrast and brightness. The number of dLGN NEUN-positive neurons and S100β-positive glial cells and those double stained with SOX2 was counted using images taken at 40X magnification from 3 sections along rostro-caudal extent of dLGN from each mouse (3 control and 3 mutant mice). Data were statistically analysed using two sample t-test ($p<0,05$) or Mann-Whitney test ($p<0,001$), after applying Shapiro-Wilk normality test.

Labelling of retino-geniculate projections

$Sox2^{Th\Delta/\Delta}$ mutants and controls were perfused (P0, P5), heads were post-fixed in PFA 4% overnight at 4°C and then washed 3 times in PBS. DiI crystals (Invitrogen) were inserted in the optic disc in one eye and then incubated at 37°C in PBS containing PFA 0.1% for 1-2 weeks essentially as

described in (Sanchez-Arrones et al., 2013). Brains were dissected, embedded in 4% agarose, sectioned with a vibratome (70µm), mounted on glass slides with Fluormount (Sigma) containing DAPI and imaged with an epifluorescence microscope (Nikon).
To label retino-geniculate projection with a different, more rapid method, $Sox2^{Th\Delta/\Delta}$ mutants and controls (P0, P7 and P21) were anesthetized and cholera-toxin subunit B (CTB) conjugated to a fluorochrome (Life Technologies) was injected in each eye, CTB-Alexa 488 (green) in the right and CTB-Alexa 594 (red) in the left eye as described in (Sanchez-Arrones et al., 2013). After 24-72 h mice were perfused, brains were dissected, embedded in 4% agarose, sectioned with a vibratome (70µm), mounted on glass slides with Fluormount (Sigma) containing DAPI and imaged with an epifluorescence or confocal microscopy (Nikon).

Labelling of cortico-thalamic projections

$Sox2^{Th\Delta/\Delta}$ mutants and controls were perfused at P8, brains were dissected, fixed in PFA 4% overnight at 4°C and then washed 3 times in PBS. DiI and DiA crystals (Invitrogen) were inserted in the primary visual and primary somatosensory area, respectively. Brains were incubated at 37°C in PFA 4% for 4 weeks and then embedded in 4% agarose, sectioned with a vibratome (70µm), mounted on slides with Fluormount (Sigma) containing DAPI and imaged with an epifluorescence microscope (Nikon). DiA staining in the VP was observed in 100% of controls and mutants while DiI staining in the dLG was observed in 60% of controls and 10% of mutants.

Quantification of projections to LG

Images were taken with a confocal microscope (Nikon), two or three central sections of each brain were analysed, stacks of 30 µm were generated for each section and Image J was used to reduce background with a rolling ball filter of 250 pixels. The LG (lateral geniculate) was thresholded in an unbiased way, using the default function of ImageJ, to generate a binary image that resembles the original unthresholded contralateral (CL) and ipsilateral (IL) projections. The percentage of CL or IL projections reaching the dLG or vLG was calculated on the thresholded images (es. area CL projections in dLG/area total CL projections in LG x 100). DAPI staining of each section was used to help define the borders of the dLG and vLG. The area of the dLG and vLG was measured on these sections with ImageJ. Data are represented as mean ± standard deviation and were statistically analyzed using unpaired Student's T-test, ** $p<0.01$, *** $p<0.005$, after applying Shapiro-Wilk normality test.

ChIP-seq

ChIPseq was performed on neural stem/progenitor cell cultures (neurospheres) obtained from six P0 forebrains (Favaro et al., 2009, Zhang et al., 2013). Briefly, cells were collected as small neurospheres and fixed sequentially with di(N-succimidyl) glutarate and 1% formaldehyde in phosphate-buffered saline and then lysed, sonicated and immunoprecipitated as described previously (Mateo et al., 2015). SOX2 was immunoprecipitated with 3 mg of goat anti-SOX2 (Santa Cruz sc-17320). DNA libraries were prepared from 10 ng of immunoprecipitated DNA and 10 ng of input DNA control, according to the standard Illumina ChIP-seq protocol. Libraries were sequenced with the Genome Analyzer IIx (Illumina). The raw reads were mapped to the mouse genome (mm9 including random chromosomes) with Bowtie version 0.12.5. We used MACS (Zhang et al., 2008) version 2.0.9 to define Sox2 bound regions (peaks). The details and global features of this SOX2 ChIPseq analysis are reported in (Bertolini et al., 2019).

Luciferase constructs

The Efna5 SOX2-bound 3' region (1178 bp) was amplified by PCR from genomic DNA with the following primers:

Forward (XhoI) 5' ATATCTCGAGTGAAACCAAATAACGGCAGACT 3' (added XhoI site underlined); Reverse (SacI) 5' ATATGAGCTCTGTAAGTCATCTAGGCATGGAGA 3' (added SacI site underlined).

The Efna5 SOX2-bound 5' region (826 bp) was amplified by PCR with the following primers:

Forward (XhoI) ATATCTCGAGGGGAGAGCGGTTATTCTGGAAC (added XhoI site underlined)

Reverse (SacI) ATATGAGCTCCTGCAATGACATTCTGGGCAGA (added SacI site underlined).

The 3' and 5' Sox2-bound regions of Efna5 were cloned upstream of the minimal TK promoter into the SacI and XhoI-digested TK-LUC vector (Mariani et al., 2012) to generate 3' peak-luciferase and 5' peak-luciferase plasmids respectively.

Transfections

Transfections were performed essentially as described in (Panaliappan et al., 2018). Neuro-2a cells ($1.5x10^5$ cells/well) were plated in 12-well plates in 1 ml of MEM (Sigma) supplemented with 10% foetal bovine serum, 1% L-glutamine, 1% penicillin and streptomycin, and transfected after 24 h with Lipofectamine^R 2000 Reagent (Invitrogen). Medium in each well was replaced with 1 ml of MEM medium (with no additions) mixed with 2 µl of Lipofectamine 2000 and DNA. We used a fixed amount of 300 ng of luciferase reporter plasmids (3'peak-Luciferase, or 5'peak-Luciferase) and increasing amounts of Sox2-expressing vector (Favaro et al., 2009). pBluescript was added to

each transfection to equalize total DNA to 800 ng. We used the Nkx2.1-luciferase construct (Ferri et al., 2013) as a positive control of Sox2 activation. We used the following molar ratios of peak-luciferase vector: Sox2 expressing vector: 1: 0.06 (+), 1:0.125 (++), 1:0.187 (+++), 1:0.250 (++++), 1:0.50 (+++++). After 24 h cells were washed with PBS and lysed with Lysis Buffer (Promega) for 20 min on a rocker. The cells were then subjected to a freeze-thaw cycle (20 min at -80°C and 20 min at 37°C) and lysates were collected and centrifuged at 4°C for 1 min at 13000 rpm. Luciferase activity was measured with the Dual Luciferase^{R} Reporter Assay System (Promega) according to the provided instructions by using the Glomax luminometer. Results, represented in histograms as percentage of luciferase activity, are the mean of three independent transfections in triplicate. Error bars represent standard deviation. The activity of Nkx2.1-luciferase co-transfected with Sox2 was set = 100%.

Supplemental References

ALFANO, C., MAGRINELLI, E., HARB, K. & STUDER, M. 2014. The nuclear receptors COUP-TF: a long-lasting experience in forebrain assembly. *Cell Mol Life Sci,* 71**,** 43-62.

ARMENTANO, M., CHOU, S. J., TOMASSY, G. S., LEINGARTNER, A., O'LEARY, D. D. & STUDER, M. 2007. COUP-TFI regulates the balance of cortical patterning between frontal/motor and sensory areas. *Nature neuroscience,* 10**,** 1277-86.

BERTOLINI, J. A., FAVARO, R., ZHU, Y., PAGIN, M., NGAN, C. Y., WONG, C. H., TJONG, H., VERMUNT, M. W., MARTYNOGA, B., BARONE, C., MARIANI, J., CARDOZO, M. J., TABANERA, N., ZAMBELLI, F., MERCURIO, S., OTTOLENGHI, S., ROBSON, P., CREYGHTON, M. P., BOVOLENTA, P., PAVESI, G., GUILLEMOT, F., NICOLIS, S. K. & WEI, C. L. 2019. Mapping the Global Chromatin Connectivity Network for Sox2 Function in Neural Stem Cell Maintenance. *Cell Stem Cell,* 24**,** 462-476 e6.

CERRATO, V., MERCURIO, S., LETO, K., FUCA, E., HOXHA, E., BOTTES, S., PAGIN, M., MILANESE, M., NGAN, C. Y., CONCINA, G., OTTOLENGHI, S., WEI, C. L., BONANNO, G., PAVESI, G., TEMPIA, F., BUFFO, A. & NICOLIS, S. K. 2018. Sox2 conditional mutation in mouse causes ataxic symptoms, cerebellar vermis hypoplasia, and postnatal defects of Bergmann glia. *Glia*.

CHOU, S. J., BABOT, Z., LEINGARTNER, A., STUDER, M., NAKAGAWA, Y. & O'LEARY, D. D. 2013. Geniculocortical input drives genetic distinctions between primary and higher-order visual areas. *Science,* 340**,** 1239-42.

FAVARO, R., VALOTTA, M., FERRI, A. L., LATORRE, E., MARIANI, J., GIACHINO, C., LANCINI, C., TOSETTI, V., OTTOLENGHI, S., TAYLOR, V. & NICOLIS, S. K. 2009. Hippocampal development and neural stem cell maintenance require Sox2-dependent regulation of Shh. *Nature neuroscience,* 12**,** 1248-56.

FERRI, A., FAVARO, R., BECCARI, L., BERTOLINI, J., MERCURIO, S., NIETO-LOPEZ, F., VERZEROLI, C., LA REGINA, F., DE PIETRI TONELLI, D., OTTOLENGHI, S., BOVOLENTA, P. & NICOLIS, S. K. 2013. Sox2 is required for embryonic development of the ventral telencephalon through the activation of the ventral determinants Nkx2.1 and Shh. *Development,* 140**,** 1250-61.

GASTON-MASSUET, C., HENDERSON, D. J., GREENE, N. D. & COPP, A. J. 2005. Zic4, a zinc-finger transcription factor, is expressed in the developing mouse nervous system. *Dev Dyn,* 233**,** 1110-5.

HORNG, S., KREIMAN, G., ELLSWORTH, C., PAGE, D., BLANK, M., MILLEN, K. & SUR, M. 2009. Differential gene expression in the developing lateral geniculate nucleus and medial geniculate nucleus reveals novel roles for Zic4 and Foxp2 in visual and auditory pathway development. *J Neurosci,* 29**,** 13672-83.

HUBERMAN, A. D., MURRAY, K. D., WARLAND, D. K., FELDHEIM, D. A. & CHAPMAN, B. 2005. Ephrin-As mediate targeting of eye-specific projections to the lateral geniculate nucleus. *Nat Neurosci,* 8**,** 1013-21.

KERJAN, G., DOLAN, J., HAUMAITRE, C., SCHNEIDER-MAUNOURY, S., FUJISAWA, H., MITCHELL, K. J. & CHEDOTAL, A. 2005. The transmembrane semaphorin Sema6A controls cerebellar granule cell migration. *Nat Neurosci,* 8**,** 1516-24.

LI, J. Y., LAO, Z. & JOYNER, A. L. 2002. Changing requirements for Gbx2 in development of the cerebellum and maintenance of the mid/hindbrain organizer. *Neuron,* 36**,** 31-43.

LIVNAT, I., FINKELSHTEIN, D., GHOSH, I., ARAI, H. & REINER, O. 2010. PAF-AH Catalytic Subunits Modulate the Wnt Pathway in Developing GABAergic Neurons. *Front Cell Neurosci,* 4.

MARIANI, J., FAVARO, R., LANCINI, C., VACCARI, G., FERRI, A. L., BERTOLINI, J., TONOLI, D., LATORRE, E., CACCIA, R., RONCHI, A., OTTOLENGHI, S., MIYAGI, S., OKUDA, A., ZAPPAVIGNA, V. & NICOLIS, S. K. 2012. Emx2 is a dose-dependent negative regulator of Sox2 telencephalic enhancers. *Nucleic Acids Res,* 40**,** 6461-76.

MATEO, J. L., VAN DEN BERG, D. L., HAEUSSLER, M., DRECHSEL, D., GABER, Z. B., CASTRO, D. S., ROBSON, P., CRAWFORD, G. E., FLICEK, P., ETTWILLER, L., WITTBRODT, J., GUILLEMOT, F. & MARTYNOGA, B. 2015. Characterization of the neural stem cell gene regulatory network identifies OLIG2 as a multifunctional regulator of self-renewal. *Genome Res,* 25**,** 41-56.

MUZIO, L., SORIA, J. M., PANNESE, M., PICCOLO, S. & MALLAMACI, A. 2005. A mutually stimulating loop involving emx2 and canonical wnt signalling specifically promotes expansion of occipital cortex and hippocampus. *Cereb Cortex,* 15**,** 2021-8.

PANALIAPPAN, T. K., WITTMANN, W., JIDIGAM, V. K., MERCURIO, S., BERTOLINI, J. A., SGHARI, S., BOSE, R., PATTHEY, C., NICOLIS, S. K. & GUNHAGA, L. 2018. Sox2 is required for olfactory pit formation and olfactory neurogenesis through BMP restriction and Hes5 upregulation. *Development,* 145.

PFEIFFENBERGER, C., CUTFORTH, T., WOODS, G., YAMADA, J., RENTERIA, R. C., COPENHAGEN, D. R., FLANAGAN, J. G. & FELDHEIM, D. A. 2005. Ephrin-As and neural activity are required for eye-specific patterning during retinogeniculate mapping. *Nat Neurosci,* 8**,** 1022-7.

SANCHEZ-ARRONES, L., NIETO-LOPEZ, F., SANCHEZ-CAMACHO, C., CARRERES, M. I., HERRERA, E., OKADA, A. & BOVOLENTA, P. 2013. Shh/Boc signaling is required for sustained generation of ipsilateral projecting ganglion cells in the mouse retina. *J Neurosci,* 33**,** 8596-607.

ZHANG, Y., LIU, T., MEYER, C. A., EECKHOUTE, J., JOHNSON, D. S., BERNSTEIN, B. E., NUSBAUM, C., MYERS, R. M., BROWN, M., LI, W. & LIU, X. S. 2008. Model-based analysis of ChIP-Seq (MACS). *Genome Biol,* 9**,** R137.

ZHANG, Y., WONG, C. H., BIRNBAUM, R. Y., LI, G., FAVARO, R., NGAN, C. Y., LIM, J., TAI, E., POH, H. M., WONG, E., MULAWADI, F. H., SUNG, W. K., NICOLIS, S., AHITUV, N., RUAN, Y. & WEI, C. L. 2013. Chromatin connectivity maps reveal dynamic promoter-enhancer long-range associations. *Nature,* 504**,** 306-10.